博士論文

論文題目　Metabolic remodeling of mitochondrial electron transport chain under hypoxia and hyponutrition in a human pancreatic cancer cell line

（低酸素・低栄養下におけるヒト膵臓癌由来細胞株の

ミトコンドリア呼吸鎖再構築による適応代謝）

氏　名　三上　貴浩

TABLE OF CONTENTS

Abstract

The tumour microenvironment is composed of various types of cells and extra-cellular components which are interacting with tumour cells. Hypoxia/hyponutrition plays a pivotal role in the formation of microenvironment. It has been reported that in such microenvironment succinate accumulates, although the exact mechanism remains unclear. In order to study the mechanism of succinate accumulation, development of an accurate, easy and fast assay method to quantify succinate concentration is essential.

Here I established a novel cycling assay system for determination of succinate concentration. Using this assay, I evaluated the intra- and extracellular succinate concentration of DLD-1, Panc-1, and HDF cells. Under hypoxia/hyponutrition, the quinol–fumarate reductase (QFR) activity of complex II (succinate:ubiquinone reductase) increases, becoming the major source of succinate accumulation. By using respiratory chain (RC) inhibitors, two major sources of electrons leading to succinate accumulation under microenvironment-mimicking condition were identified as complex I and dihydroorotate dehydrogenase (DHODH). This result suggests that under tumour microenvironment, "metabolic remodeling" occurs, in which electron flow alters from classical oxygen respiration to fumarate respiration, and that this remodeled metabolism becomes essential to support NADH re-oxidation as well as nucleotides biosynthesis.

It is known that the mitochondrial RC is the major source of cellular reactive oxygen species (ROS). Ischemia-reperfusion (IR) injury is a universal pathological event which attributes the tissue damage to the radical oxidative stress responses induced by a short period of ischemia and subsequent reperfusion. However, enzymes directly involved in ROS production are still unclear. Since succinate is known to accumulate during ischemia, which

can drive the ROS production after reperfusion, I focused the second part of my study on succinate-driven ROS production in cultured human cells. In this study, I provide the direct evidence that mitochondrial complex II, III and possibly DHODH are the responsible of highly ROS production site at 30 min following IR.

Revealing the mechanism involved in succinate accumulation as well as succinate-mediated ROS production can provide leading drug candidates for treatment of a rage of disorders including tumours and IR injury.

Keywords: SDH, succinate assay, carcinogenesis, hypoxia, microenvironment

Abbreviations

APF, aminophenyl Fluorescein

ASCT, acetate:succinate CoA-transferase

CoA, coenzyme A

CybL, large subunit of cytochrome *b*

CybS, small subunit of cytochrome *b*

DHODH, dihydroorotate dehydrogenase

DTNB, 5,5′-dithiobis-(2-nitrobenzoic acid)

ETC, electron transport chain

Fp, flavoprotein subunit

GPCR, G-protein-coupled receptor

HIF-1α, hypoxia-inducible factor-1α

hROS, highly reactive oxygen species

IC_{50}, 50% inhibitory concentration

Ip, iron–sulfur cluster subunit

IR, ischemia-reperfusion

MK, menaquinone

MKH_2, menaquinol

NADH, nicotinamide adenine dinucleotide

NADH-FR, NADH-fumarate reductase

NTB, 2-nitro-5-thiobenzoic acid

QFR, quinol–fumarate reductase

RC, respiratory chain

ROS, reactive oxygen species

SCS, succinyl-CoA synthetase

SDH, succinate dehydrogenase

SQR, succinate:ubiquinone reductase

UQ, ubiquinone

Introduction

Succinate accumulation in tumours

Mitochondria have a diversity of roles including energy generation, various signal transductions such as reactive oxygen species (ROS)-mediated signaling (*1*), and metabolism contributing to anabolism of fatty acid (*2, 3*) or pyrimidine (*4*) and catabolism of ketone body (*5, 6*) or proline (*7*). Mitochondrial dysfunction is involved in various diseases ranging from neuronal disorders such as Parkinson's disease (*8, 9*), hereditary encephalopathy (*10-12*) and glioma (*13, 14*) to ischemia-reperfusion injury in myocardial infarction or stroke (*15-17*).

Embedded in mitochondrial inner membrane are electron transport chain (ETC) complexes, namely complex I, II, III and IV (*18*). In normoxic condition, complex I and II catalyze the electron transfer from NADH and succinate, respectively, to the ubiquinone pool (*19-22*). The electrons from reduced ubiquinone (ubiquinol) are transferred to molecular oxygen via complex III, cytochrome *c* and complex IV in a process called oxygen respiration (*23-25*). In mitochondrial matrix, eight enzymes are involved in tricarboxylic acid (TCA) cycle: citrate synthase, aconitase, isocitrate dehydrogenase (IDH), α-ketoglutarate dehydrogenase (α-KGDH), succinyl-coa synthase, succinate dehydrogenase (SDH, complex II), fumarate hydratase and malate dehydrogenase (MDH) (*26-28*). Among these TCA cycle enzymes, the following four enzymes catalyze the oxidation-reduction reaction: IDH, α-KGDH, MDH and SDH. IDH, α-KGDH and MDH produce NADH while SDH produce ubiquinol as the product of their respective enzyme reaction (*29-31*). Complex I is an

important ETC enzyme responsible for re-oxidation of NADH produced by mitochondrial pathways such as TCA cycle and β-oxidation (*32-34*). SDH, also known as complex II is unique in that it is the only membrane bound enzyme of TCA cycle and the only nuclear coded complex among other ETC complexes (Fig. 1), catalyzing the reversible conversion of succinate to fumarate (*22, 35-37*). The genes of *sdha*, *sdhb*, *sdhc* and *sdhd* encode each subunits of the mitochondrial complex II: flavoprotein (Fp), iron-sulfur cluster (Ip), cytochrome *b* large (CybL) and small (CybS) subunits, respectively (*22, 38*). In addition to Complex I and II, several peripheral respiratory enzymes have been reported to shuttle electrons to the ubiquinone pool in ETC: dihydroorotate dehydrogenase (DHODH) (*39*), glycerol-3-phosphate dehydrogenase (G3PDH) (*40, 41*) , proline dehydrogenase (PRODH) (*42, 43*), sulfide:quinone oxidoreductase (SQOR) (*44*) and electron-transfer flavoprotein dehydrogenase (ETFDH) (*45*). DHODH is involved in pyrimidine *de novo* biosynthesis pathway catalyzing its fourth step which is the only redox reaction, transferring electrons from dihydroorotate to ubiquinone (*39*). It is a validated drug target for rheumatoid arthritis, an autoimmune disease, by inhibiting the proliferation of rapidly-growing activated immune cells (B and T cells), which are dependent on pyrimidine *de novo* biosynthesis (*46*). G3PDH is a tri-functional enzyme linking lipid biosynthesis, gluconeogenesis and respiratory chain by transferring electrons from glycerol-3-phosphate to ubiquinone (*41*). It was recently reported that metformin, the first-line drug for type 2 diabetes, inhibits G3PDH and consequently liver gluconeogenesis (*47*), resulting in the decrease in glucose release to blood from liver.

Proline catabolism has been indicated to drive tumour metabolic remodeling (*48, 49*), and involves PRODH which functions not only as tumour suppressor to trigger ROS-mediated apoptosis but as tumour survival factor through ATP production depending on the tumour microenvironment (*42, 43, 49, 50*). SQOR catalyzes the first step in sulfide oxidation in mitochondria, linking H_2S oxidation to the RC and to energy metabolism (*44*). ETFDH is located in the inner mitochondrial membrane (*51*) and catalyzes electron transfer from reduced ETF to ubiquinone linking oxidation of fatty acid and some amino acids to RC (*52, 53*). The mutation of this gene predisposes its carriers to newborn severe metabolic disease, multiple acyl-CoA dehydrogenation deficiency (*45, 53-56*).

A role for mitochondria in tumour formation is implied by the fact that several tumour cells harboring mutations in the genes that encode enzymes of the TCA cycle such as isocitrate dehydrogenase (*idh*) (*57, 58*), succinate dehydrogenase (*sdh*) (*14, 59*) and fumarate hydratase (*fh*) have been reported (*11*). Point mutations in R132 in IDH gene found in several tumour cells, cause the gain-of-function in which α-ketoglutarate, the product of wild type IDH, is oxidized by NADH causing accumulation of 2-oxoglutarate, a well-known oncometabolite (*60*). SDH and FH have been suggested to act as tumour suppressor enzymes since mutation in their genes was associated to accumulation of succinate and fumarate, respectively (*14, 19, 46*), inhibiting prolyl hydroxylase enzymes resulting in stabilization of hypoxia-inducible factor-1 (HIF1α) promoting glycolysis and angiogenesis, both of which are survival responses to hypoxia in normal and malignant tissues (*61-64*).

There are also some direct evidences which shows succinate's promotive effect on proliferation of mammalian cells via a type of G-protein-coupled receptor (GPCR), GPR91 (*65*). Understanding *sdh*-related tumourigenesis is crucial, because the presence of a germline *sdhb* mutation is associated with a high risk of malignancy and a poor prognosis in paraganglioma or pheochromocytoma patients (*14, 66*). Dominant mutations in *sdhb*, *sdhc* and *sdhd* predispose carriers to carotid body paragangliomas, adrenal gland pheochromocytomas, and gastrointestinal stromal tumours (*11, 61*). These clinical facts have rendered *sdh* genes one of the most important tumour suppressor genes in recent years (*26, 62*).

From these results, it is inferred that accumulated succinate resulted from impaired succinate–ubiquinone reductase (SQR) activity of complex II contributes to the tumourigenesis in *sdh*-mutated cancer cells. My hypothesis is that this holds true even in cancer cells without *sdh* mutation growing under tumour microenvironment. In oxygen respiration, complex II functions as SQR catalyzing the oxidation of succinate to form fumarate using ubiquinone as acceptor of reducing equivalent (*29, 67*). I hypothesized that under 1% O_2/glc(-)gln(-) conditions, the SQR activity of complex II to form fumarate from succinate declines while its quinol-fumarate reductase (QFR) activity to form succinate from fumarate increases and that succinate accumulated in this process facilitates cellular survival and proliferation. Tomitsuka *et al.*, examined human cancer cells cultured under tumour microenvironment-mimicking conditions, and concluded that the

NADH-fumarate reductase (NADH-FR) system, namely "fumarate respiration" functions in the cancer cells, which is composed of complex I and QFR activity of complex II (*68, 69*). Fumarate respiration has been reported in bacteria such as *Escherichia coli* (*70*) and *Mycobacterium tuberculosis* (*71*) and also in several parasites living under hypoxic condition (*69*). It has recently been reported that menaquinone (MK) is produced by cleavage of the phytyl side chain from dietary phylloquinone to release menadione in the intestine, followed by delivery of menadione to tissues where it is converted to MK again by a prenyltransferase such as UbiA prenyltransferase domain-containing protein 1 (UBIAD1) (*72*). In fumarate respiration, reduced form of MK (low potential quinone), *i.e.*, menaquinol (MKH_2) is supposed to work as electron donor.

At present, no biochemical mechanisms for succinate accumulation in cancer cells have been provided. Neither do we have an accurate, easy nor fast assay method for succinate concentration determination since mass spectrometry is a time-consuming and expensive method for this purpose. I therefore developed an accurate, easy and fast assay system for succinate concentration using purified recombinant acetate:succinate CoA transferase (ASCT) from *Trypanosoma brucei*, the causative agent of sleeping sickness, and examined the mechanism as to how cancer cells accumulate succinate. ASCT is a mitochondrial enzyme involved in acetate fermentation found in several parasites living under hypoxic condition such as *Trypanosoma spp.* (*73*), *Leishmania spp.* (*73*), *Blastocystis sp.* (*74*), *Trychomonas vaginalis* (*75*) and helminths such as *Ascaris suum* and *Fasciola hepatica* (*76*).

In these parasites, acetate is produced from acetyl-CoA by either acetyl-CoA hydrolase (ACH) or an organellar ASCT (*77*). The ACH reaction is not coupled to ATP synthesis, whereas the ASCT reaction yields succinyl-CoA for ATP formation *via* succinyl-CoA synthetase (SCS), which is called ASCT/SCS cyclic reaction (*77*). SCS is the only mitochondrial enzyme capable of ATP production via substrate level phosphorylation in the absence of oxygen and catalyzes the following reaction:

NDP + Pi + succinyl-CoA ⟷ NTP + succinate + CoA

where NDP and NTP are purine nucleotide di- and triphosphates, respectively (*78, 79*).

This parasitic ASCT/SCS cyclic reaction has led me to establish the ASCT/SCS succinate cycling assay. Using this new assay method, the hypothesis that succinate accumulates in cancer cells and promotes cellular proliferation was tested through three experiments. In the first experiment, the effect of succinate on cellular proliferation under normoxia and hypoxia was examined. In the second experiment, I evaluated the effect of normoxia, hypoxia, nutrient-rich and -deprived conditions on intra- and extracellular succinate concentration of DLD-1, Panc-1 and HDF cells. In the third experiment, succinate level in the presence of ETC inhibitors was measured in order to identify the source of electrons flow to ETC, under 21% O_2/glc(+)gln(+) and 1% O_2/glc(-)gln(-) conditions.

ROS production after ischemia-reperfusion injury

A diversity of disorders involve overproduction of ROS, including neurodegenerative diseases

(*8, 80*), cancer (*81-85*), diabetes (*86-89*), and ischemia-reperfusion (IR) injury (*90-92*) in myocardial infarction or stroke. Of these pathologies, ischemia-reperfusion injury underlies a variety of ischemic disorders which occurs when blood supply to a certain tissue is disrupted and deteriorate the tissue damage as is notably seen following the reperfusion for liver transplantation (*93*), hepatectomy (*94*), heart attack (*95*), stroke (*96*) and acute kidney injury (*97*). Although reperfusion of ischemic tissue is essential for survival, it not only triggers inflammation due to the chemotaxis of neutrophil but also results in excess oxidative damage.

It has been suggested in previous reports that the two major ROS producing sites during cardiac IR injury are mitochondrial complex I and complex III of the mitochondrial ETC (*15, 98*).

ROS includes hydrogen peroxide (H_2O_2) and superoxide ($O_2^{\cdot -}$). Dismutation of $O_2^{\cdot -}$ produces H_2O_2 which dissociates into two hydroxyl radical ($OH^{\bullet}$) groups that react with guanine to form 8-oxoguanine (*99*) leading to mutagenesis and finally to irreversible cellular damage. A number of studies have already been reported linking ROS (mainly superoxide) production to IR injury (*100-107*). It has been reported that during IR, superoxide is generated at complex I (*108*), although the production site of other ROS, especially highly ROS (hROS) which are the most reactive form of ROS, *i.e.*, hydroxylradical ($OH^{\bullet}$) and peroxynitrite ($ONOO^-$), remains unclear.

The aim of the study as is mentioned in chapter 2 is to gain deeper insights into hROS

production site in IR-mimicking condition which may be a potential therapeutic target for IR injury. To attain this purpose, I focused on hROS and investigated its production site. In this report, I provide the biochemical evidences that mitochondrial complex II, III and possibly DHODH are the responsible hROS production site at 30 min following IR-mimicking condition.

Because increasing reports have indicated the importance of succinate (*108, 109*) and mitochondrial complex II in IR (*108, 110-112*), I also focused on the succinate accumulation during IR-mimicking condition using my novel succinate cyclic assay system. As result, I provided evidence that under ischemic condition, QFR activity of complex II to form succinate from fumarate increased and succinate produced in this process directly fuels hROS production during reperfusion. I also showed that production of hROS during reperfusion can be suppressed in the presence of complex II, III and DHODH inhibitors. Revealing the mechanism involved in succinate-mediated hROS production is of great importance for development of therapeutics for a diversity of disorders associated with this process.

Chapter 1. Metabolic remodeling of mitochondrial electron transport chain under hypoxia and hyponutrition

1-1. Material and Methods

Reagents

Sodium chloride, magnesium chloride, rotenone, atpenin A5, dimethyl malonate, antimycin A, brequinar sodium and Aminophenyl Fluorescein were purchased from Sigma. Hoechst 33258 was purchased from Molecular Probes. Glutathione was purchased from Wako. Ferulenol was purchased from Santa Cruz Biotechnology. The chemical structures of mitochondrial complex inhibitors (rotenone, atpenin A5, antimycin A, brequinar, ferulenol and A771726) are shown in appendix.

ASCT/SCS succinate cycling assay

The expression and purification of *T. brucei* ASCT have been established by Dr. D. K. Inaoka (unpublished). The gene coding for TbASCT (Tb927.11.2690) was amplified from ILTat 1.4 strain genomic DNA, inserted into pET151-TOPO vector and used to transform *E. coli* TOP10 chemically competent cell (Invitrogen). Positive colonies were selected under 100 μg/mL carbenicillin. Five mL LB culture of positive colonies were cultured overnight, the plasmid purified by MagExtractor (Takara) and confirmed by sequencing. The resultant plasmid (pET151/TbASCT) was introduced into *E. coli* BL21star(DE3) strain for expression and purification. The best expression condition was achieved by culturing BL21star(DE3)

pET151/TbASCT at 20˚C in 500 mL TB medium shaking at 200 rpm for 16 hours without addition of IPTG. All of following procedures were conducted at 4˚C. The cells were harvested at 3000 × *g* for 10 minutes, suspended in 60 mL of lysis buffer [50 mM Tris-HCl pH 8.0, 20% (v/v) glycerol, 1 mM EDTA, 300 mM NaCl, 10 mM $MgCl_2$ and 0.25 mM PMSF] supplemented by 10 mM imidazol and broken by French press at 180 MPa. Cell debris and unbroken cells were removed by centrifugation at 30,000 × *g* for 30 minutes and the soluble fraction obtained by collecting the following ultracentrifugation at 200,000×*g* for 2 hours. The soluble fraction containing TbASCT was applied into 3 mL of Ni-NTA (Qiagen) column pre-equilibrated by lysis buffer. TbASCT was purified by consecutively washing the column by 60 mL of lysis buffer containing 70, 100 and 250 mM imidazol at a flow rate of 1 mL/min and 1.5 mL/fraction collected. Active fractions were pooled and concentrated by Vivaspin 50 kDa MWCO. For storage, 100% glycerol was added to final 50% (v/v) and kept at -20˚C until use.

The succinate cycling assay consisted of 100 mM Tris-HCl, 2 mM $MgCl_2$, 0.1% (v/v) TritonX-100, 2 mM NaPi, 1 mM ADP, 100 μM 5,5'-dithiobis-(2-nitrobenzoic acid) (DTNB), 0.5 mM acetyl-CoA, and 1.1 U/mL SCS (purchased from MEGAZYME) and 250 ng/mL purified TbASCT (reaction mix) in presence of succinate and followed the increase in absorbance at 412 nm due to 2-nitro-5-thiobenzoic acid (NTB) production. Standard curve of succinate concentration was calculated in each assay by transferring reaction mix into 96-well plate containing varying concentration of succinate. Absorbance slope was defined as the slope

(Abs/min) between 3.5 min and 10 min in the TbASCT/SCS activity graph (Fig. 4) and succinate concentration was calculated from the standard curve.

Cell culture

DLD-1, Panc-1, human dermal fibroblast (HDF) cells were provided from Taiho Pharmaceutical Company (Japan) and cultured in DMEM (Invitrogen) containing high glucose levels (4.5 g/L), supplemented with 10% (v/v) heat-inactivated fetal bovine serum (FBS, GIBCO BRL) adjusted to pH 7.4 in a humidified atmosphere at 37°C, 5% CO_2 and 21% O_2 (mimicking normoxia) in a CO_2 incubator ACI-165D (ASTEC). DLD-1 is a colorectal adenocarcinoma cell line and Panc-1 a pancreatic epithelioid carcinoma cell line. These cell lines are here used as an *in vitro* model of cancer cells. HDF is a human dermal fibroblast cell line and was used as a model of normal cells.

Hypoxia/hyponutrition conditions were attained by exposure to 1% O_2 and 5% CO_2 in a humidified incubator MG-70M (TAITEC) and culture in DMEM without FBS, glutamine or glucose (1% O_2/glc(-)gln(-) conditions).

To analyze the origin of electron flow from ETC causing accumulation of succinate, cultured cells were exposed to inhibitors of complexes I (rotenone), II (atpenin A5), III (antimycin A) and DHODH (ferulenol).

Cultured medium and ethanolic extract from the cells

DLD-1 cells were seeded at 1.0×10^6, 2.0×10^6, 4.0×10^6, 6.0×10^6 /mL in 96-well plates under 21% O_2/glc(+)gln(+) and 1% O_2/glc(-)gln(-) conditions. After incubation for 48 hr at 37°C, the medium was transferred to another well and the cells were washed with PBS and treated with 100% ethanol. These procedures were done within 5 minutes. The ethanolic extract was transferred to another well to be evaporated and then medium for each condition was added into distinct well. This ethanolic extract and medium was used as the sample for ASCT/SCS succinate cycling assay, the absorption slope of which indicates the intra- and extracellular succinate concentration, respectively.

Viability assay

DLD-1 and Panc-1 cells were seeded at 1.0×10^3 /mL in 96-well plates under 21% O_2/glc(+)gln(+) and 1% O_2/glc(-)gln(-) conditions. After incubation for 24 hr at 37°C, succinate or various ETC inhibitors were added. These cells were incubated for another 24 hr and then cell viability was evaluated by counting cell numbers. The relative proliferation rate was calculated by dividing the cell number of the well of interest by that of the well untreated.

Mitochondria preparation

Preparation of mitochondria from cultured cells was performed as previously described (*113*). Briefly, cultured cells were suspended in mitochondrial preparation buffer containing 250 mM sucrose, 20 mM HEPES, 3 mM EDTA and 1 mM sodium malonate at pH 7.5. Cell

suspension was homogenized by 50 strokes using a Potter-Elvehjem Teflon-pestle homogenizer. The volume of the homogenate was adjusted to 10 mL by the addition of mitochondrial preparation buffer, and centrifuged at 500 × *g* for 15 min at 4°C to remove cell debris and nuclei. The supernatant was centrifuged at 14,300 × *g* for 15 min at 4°C to precipitate the mitochondria. The pellet was resuspended in mitochondrial preparation buffer and centrifuged at 14,300 × *g* for 15 min at 4°C. Finally, this pellet was suspended in mitochondrial preparation buffer without malonate for use as the mitochondrial fraction.

Statistical Analysis

Quantitative data were expressed as the means ± standard deviation. Statistical analyses were performed using Student's t test or a one-way ANOVA followed by a Fisher protected least significant difference (PLSD) post-hoc test. Values of $p < 0.05$ were considered statistically significant.

1-2. Results

Effect on the proliferation rate of adding succinate to the medium

The fact that mutations of *sdh* genes promote carcinogenesis (*26, 61*) implies the facilitative effect of succinate on cellular proliferation. Thus, I hypothesized that addition of succinate to the culture medium would promote the proliferation of DLD-1 and Panc-1. Indeed, addition of 10 μM or more succinate to the medium promoted the proliferation of Panc-1 cells under 1% O_2/glc(-)gln(-) condition at 12 hr after incubation but not for DLD-1 cells (Fig. 2). In contract, this effect was not observed under 21% O_2/glc(+)gln(+) condition (Fig. 2). In this experiment, it was concluded that the proliferative effect of succinate was cell-line specific and only seen under 1% O_2/glc(-)gln(-) condition. This result suggests that succinate accumulation may be involved in carcinogenic process.

Establishment of the assay method for succinate concentration

Succinate is involved in various pathological events including ischemia-reperfusion injury in myocardial infarction (*108*) or angiogenesis in diabetic retinopathy (*114*). Such a simple method to measure succinate concentration as can be used in clinical is in urgent demand. I established a novel succinate assay method using ASCT and SCS and named it ASCT/SCS succinate cycling assay and confirmed the accuracy of this assay system (Fig. 3).

ASCT is an acetate-producing enzyme shared by mitochondria of trypanosomatids and anaerobically functioning mitochondria (*74*). It produces acetate and succinyl-CoA from

acetyl-CoA and succinate. SCS converts succinyl-CoA into succinate and CoA in the presence of ADP and Pi (*78*). This enzyme is highly specific for its substrate succinyl-CoA (*78*). With enough acetyl-CoA and ADP, these two enzymes continuously produce CoA, and the speed of this reaction depends on the concentration of succinate (Fig. 3). In the presence of DTNB, CoA reduces DTNB into NTB (Fig. 3). Samples may well include succinyl-CoA, but succinyl-CoA is a high-energy compound and therefore should be scarce compared to succinate, which indicates that the influence of succinyl-CoA in samples is negligible.

In this ASCT/SCS succinate cycling assay, the absorbance slope used to calculate succinate concentrations was defined as the NTB production activity from the most linear region (between 3.5 and 10 min) in the activity curve (Fig. 4), where high correlation was observed between succinate concentration and the absorbance slope. At the concentration of 250 and 750 ng/mL of ASCT and 1.1 U/mL of SCS, the correlation coefficient was $R^2 = 0.9974$ and 0.9997, respectively, and the minimum limit of determination of succinate was 0.01 mM ($p < 0.0001$) in both ASCT concentrations tested (Fig. 5).

Because the high correlation was reproducibly observed between succinate concentration and the absorbance slope, this assay method was proven to be efficient and specific. This assay is a cycling assay and lowest concentration of succinate can react cyclically to form detectable NTB, by increasing the reaction time. All the following experiments were done under 1.1 U/mL of SCS and 250 ng/mL of ASCT, because the minimum limit of determination of succinate was the same for 750 ng/mL of ASCT.

Evaluation of intra- and extracellular succinate concentration

There have been several reports that refer to intra- and extracellular succinate concentration, but the intracellular concentration of succinate differs among the reports and ranges from 10 μM (*115*) to 1 mM (*116, 117*). Therefore I analyzed the succinate concentration by ASCT/SCS succinate cycling assay.

Using the succinate standard curve (see Methods), intra- and extracellular amount of succinate per cell was calculated (Fig. 6) using DLD-1 and Panc-1 cells. Under nutrient-deprived conditions, intracellular succinate concentration was higher than that of nutrient-rich conditions reaching the highest value under hypoxia/nutrient-deprived conditions in both cancer cell lines (Fig. 6A-1, 6B-1). If the volume of cell is taken into account (*118*), the intracellular concentration of succinate could be estimated to be 1 mM, which was consistent with the previous report (*119*).

Under 1% O_2/glc(-)gln(-) condition, the DLD-1 and Panc-1 cells secreted significantly higher level of succinate to the extracellular compartment reaching higher values than the other conditions (Fig. 6A-2, 6B-2). In both cells, hypoxia and hyponutrition had additive effect on succinate accumulation in the medium (Fig. 6A-2, 6B-2).

Effect of ETC inhibitors and DHODH inhibitors on succinate concentration

To identify the origin of electrons in ETC flow to succinate, I measured intra- and

extracellular succinate concentration in 21% O_2/glc(+)gln(+) conditions and in 1% O_2/glc(-)gln(-) conditions with inhibitors of complex I (rotenone), complex II (atpenin A5) and complex III (antimycin A) added in the medium.

DHODH is an enzyme which oxidizes dihydroorotate (DHO) to form orotate (ORO) and facilitates *de novo* pyrimidine biosynthesis pathway (*4, 39, 46, 120, 121*). Under 1% O_2/glc(-)gln(-) conditions, pyrimidine biosynthesis is totally dependent upon the *de novo* pathway, because pyrimidine intermediates are depleted and the salvage pathway does not work (*120, 122-124*). Brequinar, an anticancer compound, and immunosuppressive compound A771726 are also shown to inhibit DHODH (*4, 46*). Recently, our group found that ferulenol, a natural compound isolated from the Mediterranean perennial herb, *Ferula communis*, inhibited human DHODH at IC_{50} of 138 nM. In this study, I also examined the cytotoxic effects of these DHODH inhibitors on cancer cells under 21% O_2/glc(+)gln(+) conditions and 1% O_2/glc(-)gln(-) conditions. In addition, the succinate level of the cells treated with these compounds was also examined by the ASCT/SCS succinate cycling assay in order to elucidate the function of complex II.

In DLD-1 cells, in 21% O_2/glc(+)gln(+) conditions, addition of atpenin A5 significantly increased the intra- and extracellular succinate level (Fig. 7A). Addition of rotenone did not change the succinate level in 21% O_2/glc(+)gln(+) conditions (Fig. 7A). These results indicate that in 21% O_2/glc(+)gln(+) conditions, complex II acts as SQR and that electron obtained by oxidizing succinate flows from complex II to complex III via ubiquinone.

In DLD-1 cells, in 1% O_2/glc(-)gln(-) conditions, succinate level remained unchanged by adding antimycin A, whilst addition of atpenin A5 significantly lowered extracellular succinate level from 33.3×10^{-16} mol/cell to 12.9×10^{-16} mol/cell (Fig. 7B). This indicates that in 1% O_2/glc(-)gln(-) conditions, complex III does not transport electrons to cytochrome *c* but electrons flow from upstream pathways to complex II, converting fumarate to succinate via MK. This is consistent with the result that addition of rotenone decreased extracellular succinate concentration from 33.3×10^{-16} mol/cell to 26.8×10^{-16} mol/cell (Fig. 7B), indicating that electrons from complex I flow to complex II by its QFR activity in 1% O_2/glc(-)gln(-) conditions (Fig. 1). The fact that in DLD-1 cells rotenone did not significantly reduce the succinate accumulation to atpenin A5 level (Fig. 7B) strongly indicate the existence of electron donor other than complex I. Addition of ferulenol, a DHODH inhibitor, did not change succinate level in 21% O_2/glc(+)gln(+) conditions (Fig. 7A), while in 1% O_2/glc(-)gln(-) conditions it reduced the extracellular succinate concentration from 33.3×10^{-16} mol/cell to 28.4×10^{-16} mol/cell (Fig.7B). In 1% O_2/glc(-)gln(-) conditions, concomitant addition of rotenone and ferulenol decreased even more the extracellular succinate concentration to the level lower than addition of individual inhibitor, but to the level similar to atpenin A5 treatment (Fig. 7B). These results revealed that in 1% O_2/glc(-)gln(-) conditions, in addition to complex I, electrons from DHODH are transferred to complex II to reduce fumarate into succinate. This shows that in DLD-1 cells, complex I and DHODH are the two main electron donors to succinate production by complex II in 1% O_2/glc(-)gln(-) conditions (Fig. 1).

In DLD-1 cells, in 21% O_2/glc(+)gln(+) conditions, addition of antimycin A had a tendency to increase extracellular succinate ($p > 0.05$; not significant), but not to the level by atpenin A5 (Fig. 7A); this fact means that electron from complex II possibly leaks between complex II and III when complex III is inhibited. This is reasonable since inhibition of complex II (*125, 126*) or III (*127*) was reported to cause production of ROS.

In Panc-1 cells, the same tendency was observed as in DLD-1 cells (Fig. 7C, D), except that in Panc-1 cells cultured under 1% O_2/glc(-)gln(-) conditions, addition of rotenone and ferulenol lowered the succinate level to atpenin A5 level ($p < 0.05$, Fig. 7D), whilst in DLD-1 it did not ($p > 0.05$, Fig. 7B), raising the possibility that another electron donor, such as SQOR, G3PDH, PRODH and ETFDH, still might be involved in succinate production by complex II in DLD-1 cell (Fig. 1).

In HDF cells, the succinate level did not decrease by atpenin A5 treatment under 21% O_2/glc(+)gln(+) and 1% O_2/glc(-)gln(-) conditions (Fig. 7E, F), which suggests that in normal cells, unlike cancer cells, complex II does not act as QFR at least under conditions tested in this study.

Inhibitory effects of ferulenol and atpenin A5 on cellular proliferation

To examine if DHODH inhibitors and atpenin A5 are 1% O_2/glc(-)gln(-)-condition-specific, anti-proliferative effect of these compounds in 21% O_2/glc(+)gln(+) and 1% O_2/glc(-)gln(-) conditions were analyzed. As DHODH inhibitors, ferulenol and brequinar were used in this

experiment. Ferulenol, brequinar, and atpenin A5 inhibited the proliferation of DLD-1 cells at IC_{50}s of 5.6, 63.7 and 15.3 μM, respectively, in 1% O_2/glc(-)gln(-) conditions, whereas these inhibitors have an IC_{50} of more than 100 μM in 21% O_2/glc(+)gln(+) conditions (Fig. 8A). The same tendency was observed in Panc-1 cells: ferulenol, brequinar, and atpenin A5 inhibited the proliferation of Panc-1 cells at IC_{50}s of 2.8, 83.4 and 1.3 μM, respectively, in 1% O_2/glc(-)gln(-) conditions, whereas these inhibitors have an IC_{50} of more than 100 μM in 21% O_2/glc(+)gln(+) conditions (Fig. 8B), suggesting that these drugs can specifically inhibit the proliferation of cancer cells in 1% O_2/glc(-)gln(-) conditions.

1-3. Discussion

The tumour microenvironment is composed of various types of cells such as stromal fibroblasts (*128*), endothelial cells (*129*) , immune cells (*130, 131*), etc. and extra-cellular factors such as cytokines (*132-134*), growth factors (*135, 136*), extracellular matrix (*137-139*), hypoxia (*140, 141*), etc. which are interacting with tumour cells. The microenvironment not only plays an important role in tumour initiation, progression, and metastasis but has tremendous effects on therapeutic efficacy (*142, 143*). Among these elements, the study here especially focused on hypoxia/hyponutrition. A major determinant, which links the tumour microenvironment with succinate accumulation, is the physiological oxygen concentration in the tumour microenvironment. While experiments which examine the tumour microenvironment *in vitro* are mostly investigated under 21% O_2, the 'physiological' oxygen concentration in the tumour microenvironment is usually far below 10%, even around 1% (*144*). Large areas of tumour are, therefore, nutrient-deprived. Momose *et al.*, reported that efrapeptin F, a mitochondrial complex V inhibitor had preferential cytotoxicity to nutrient-deprived Panc-1 cells compared with nutrient-rich Panc-1 cells (*145*), suggesting the importance of mitochondrial metabolism in cancer cells specifically in nutrient-deprived conditions.

Succinate plays a pivotal role in a series of disorders and contributes much to their pathologies (*26, 65, 114, 146*). Because the intra- and extracellular concentration of succinate can be very low (*115, 116*), highly sensitive and specific methods for determining succinate

levels are required. I established a specific, rapid, and reproducible assay system for succinate concentration named "ASCT/SCS succinate cycling assay." This method is unique in that it is a cycling assay and because of this, is more sensitive than conventional ones. Using this assay, I evaluated the intra- and extracellular succinate concentration of DLD-1 and Panc-1 cells under 21% O_2/glc(+)gln(+) and 1% O_2/glc(-)gln(-) conditions. Under 1% O_2/glc(-)gln(-) conditions, DLD-1 and Panc-1 cells secreted more succinate than under 21% O_2/glc(+)gln(+) conditions, suggesting that 1% O_2/glc(-)gln(-) conditions induce those cells to produce and secrete succinate. Here I suggest that accumulated succinate also contributes significantly to the tumour microenvironment.

There are two types of complex II in human mitochondria, type I (complex II^I) and type II (complex II^{II}) with two different Fp subunits (*17*). The apparent K_m values for succinate of complex II^I and complex II^{II} at pH 8.0, which is the optimal pH for complex II^I, were 210 ± 80 μM and 750 ± 140 μM, respectively (*17*). These K_m values were within the succinate concentration measured in the method here.

From the experiments of ETC inhibitors, it has been revealed that in 1% O_2/glc(-)gln(-) conditions complex II acts as QFR. The QFR catalyzes the reverse reaction of the normoxic SQR reaction, resulting in succinate accumulation under 1% O_2/glc(-)gln(-) conditions. In this condition, electrons from complex I by oxidizing NADH are transferred to complex II, where its QFR activity reduces fumarate to succinate. This is believed to be an adaptive cellular mechanism to produce ATP in the absence or in the presence of low concentration of oxygen.

I also demonstrated that in 1% O_2/glc(-)gln(-) conditions, electrons produced by DHODH also flow to complex II, making possible the biosynthesis of pyrimidine even in the absence of oxygen. In 1% O_2/glc(-)gln(-) conditions, the contribution of complex I and DHODH as electron donors to QFR activity of complex II is comparable to each other, and they can be two main electron donors.

Chapter 2. Highly reactive oxygen species is generated at complex II and III following ischemia-reperfusion-mimicking treatment due to accumulation of succinate under acidic conditions.

2-1.Material and Methods

Cell culture, IR-mimicking treatment protocol

Panc-1 cells and human dermal fibroblast (HDF) cells were provided from Taiho Pharmaceutical Company (Japan) and were cultured in DMEM (Invitrogen) containing high glucose levels (4.5 g/L), supplemented with 10% (v/v) heat-inactivated fetal bovine serum (FBS, GIBCO BRL) in a humidified atmosphere at 37°C, 5% CO_2 and 21% O_2 (normoxia) in a CO_2 incubator ACI-165D (ASTEC). These cells have already been examined for succinate level and I used these cells as a model for IR-injured cells. Panc-1 is a pancreatic epithelioid carcinoma cell line and was used here as an *in vitro* model of cancer cells. HDF is a human dermal fibroblast cell line was used as a model of normal cells. Hypoxic condition was attained by exposure to 1% O_2 and 5% CO_2 in a humidified incubator MG-70M (TAITEC).

Cardiac ischemia is accompanied by a gradual decrease in cellular pH that can reach to even as low as 6.0 with prolonged ischemia time (*147*). To mimic this acidic condition, the pH of culture medium was adjusted to 6.9 by adding phosphate buffer, and the experiment was done under either pH 6.9 or pH 7.4.

Cells were seeded at 1.0×10^6 /mL in Chamber Slide™ (Sigma) and incubated under normoxia for 24 hours. These cells underwent the following protocol which aimed to mimic

IR condition. Cells were first transferred to hypoxic condition and incubated for another 30 minutes (mimicking ischemia). At the end of hypoxic period, various inhibitors of ETC were added and then the cells were re-incubated in normoxia for 20 minutes, 30 minutes, 1hour, and 2 hours (mimicking reperfusion) (Fig. 9).

hROS Production Measurement

Aminophenyl Fluorescein (APF) is reported to be highly selective for hROS with its fluorescence not being changed in the presence of H_2O_2 (*148*). Five μM of APF and 1 μg/mL of Hoechst 33258 (Molecular Probes), as indicators of hROS and nuclei respectively, were added to cultured cells at the time course described above after the onset of normoxia. The reaction was allowed to proceed at 37 °C for 30 minutes. The residual dye was washed out with PBS and the cells observed using a Zeiss Axio Imager.M2 microscope equipped with an EC Plan-Neofluar 40x/0.75 M27 objective. The exposure time was 1000, 50 and 40 msec for GFP, Hoechst and brightfield, respectively. 38 HE Green Fluorescent Prot was used as a reflector. The imaging of Hoechst 33258 and APF was achieved by excitation at 405 nm and 490 nm, and the emissions were collected at 450nm and 515nm, respectively. All the experiments were done within five minutes.

Analog signals were digitized (Image J) for analysis using MATLAB (The MathWorks, Natick, MA) and Excel (Microsoft, Redmond, WA) software.

Inhibitors of ETC

To elucidate the ROS production site in ETC, cultured cells were exposed to inhibitors of mitochondrial electron flow at the level of complexes I (5 μM rotenone), II (5 μM atpenin A5, 5 mM dimethyl malonate) and III (5 μM antimycin A).

Rotenone and atpenin A5 bind at the ubiquinone binding site and inhibit transfer of electrons from NADH or succinate to ubiquinone in complex I (*149, 150*) or II (*151, 152*), respectively. Dimethyl malonate inhibits complex II at its FAD site by competing with succinate or fumarate (*153, 154*). Antimycin A inhibits complex III at its ubiquinone binding site (*155*) near the matrix side of the inner membrane (Q_i) but not Q_o site.

Dihydroorotate dehydrogenase (DHODH) is an enzyme which oxidizes dihydroorotate to orotate, the fourth step in pyrimidine *de novo* biosynthesis pathway. In chapter 1, I have demonstrated that, electrons produced in this oxidation process flow to complex II during 1% O_2/glc(-)gln(-) conditions using ferulenol, a natural compound isolated from the Mediterranean perennial herb, *F. communis* which inhibits DHODH at IC_{50} of 138 nM. In addition to complexes I, II and III inhibitors, the hROS and succinate levels of the cells treated with ferulenol were also evaluated. These inhibitors were added to the culture medium immediately after the hypoxic period (at the time point of 2 in fig. 9), and the cells were analysed for its hROS and succinate level after another 30 min of normoxia (at the time point of 4 in fig. 9) (Fig.10).

2-2. Results

Time course of ROS production and medium succinate level

To investigate when hROS is most generated after IR-mimicking condition, the hROS level was analysed at various time-points (20 min, 30 min, 1 h, 2 h) after 30-min of hypoxia. In Panc-1 cells, the hROS level continued to rise until 30 min, when it reached its peak, and continued to decline after 30 min irrespective of the pH (Fig. 11). Large increase of hROS production was observed at pH 6.9 rather than at pH 7.4. Similar pattern was observed in HDF cells at pH 6.9 while at pH 7.4 the hROS level showed only a modest increase 30 min after IR-mimicking treatment (Fig. 11).

Along with this result, hypoxic stimuli elevated the succinate level of the culture medium to as high as 31.3×10^{-16} mol/cell and 47.1×10^{-16} mol/cell for Panc-1 and HDF, respectively, at the end of 30 min of hypoxic period under pH 6.9 (Fig. 12A). In Panc-1, at pH 7.4, significant succinate accumulation was observed during hypoxic period ($p < 0.05$, Fig.12A), while in HDF, at pH 7.4 no significant change in succinate amount was observed ($p > 0.05$, Fig. 12A).

From these results, it was concluded that in HDF, both hypoxia and acidic condition (pH 6.9) are essential factors for complex II to work as QFR producing succinate, although in Panc-1 cells hypoxia alone can induce succinate production (Fig. 13). Interestingly, accumulated succinate (at time point 3) was completely consumed within 20 min (at time point 3) indicating considerable high electron flow from complex II to RC during reperfusion-mimicking condition (Fig. 12A).

Then, succinate level in dimethyl malonate-treated group and antimycin A-treated group was each measured (Fig. 12B, C). Both in Panc-1 and HDF cells, dimethyl malonate inhibited the consumption of succinate during reperfusion-mimicking condition (time point 3 to 6 in Fig. 12B and C). In the same experiment, antimycin A also inhibited succinate consumption consistently with the previous experiments (Fig. 7A, C), by stopping the electron flow from succinate to III.

hROS production site during IR-mimicking condition at pH 6.9

Because it has been reported that ROS production is driven by succinate (*108*), I analyzed hROS production site during IR-mimicking condition at pH7.4 and 6.9 (Fig. 14). Fluorescence level of APF was analysed by microscope for hROS level at the time point of 4 in fig. 9, *i.e.*, after 30-min normoxia following hypoxia. When 5 mM glutathione, hROS scavenger, were added to the medium at the end of hypoxic period (Fig. 14), it significantly reduced hROS production, confirming that the fluorescent intensity of APF is mediated by hROS production.

To analyze hROS production site in IR-mimicking condition, inhibitors for mitochondrial ETC enzymes were used. To mimic physiological acidemia reported during *in vivo* IR, the experiment here was also done at pH 6.9 (Fig. 14) and the result obtained was compared to pH 7.4.

Panc-1 and HDF cells showed significantly lower hROS production level when treated

with 5 mM dimethyl malonate (Fig. 14), indicating that in IR-mimicking condition most of hROS is being produced by the flow of electron generated at complex II, most likely by re-oxidizing succinate which had been accumulated during hypoxic period. Consistently, comparable hROS production with that of IR-mimicking group was observed with treatment of 38.2 μM dimethyl succinate under normoxia which was the estimated succinate concentration by ASCT/SCS cycling assay after 30 min exposure to hypoxia. Atpenin A5 (5 μM) treatment did not reduce hROS level to the dimethyl malonate level, meaning that significant amount of hROS are produced at either the FAD or [Fe-S] subunit of complex II. In Panc-1 cells, rotenone (5 μM) treatment did not reduced hROS production compared to the control group, leaving little possibility of hROS production from complex I at least 30 min after IR-mimicking condition. Atpenin A5 (5 μM) treatment did not reduce hROS level to the dimethyl malonate level. Therefore, the decrease in hROS production caused by atpenin A5 treatment compared to the inhibition control (dimethyl malonate) can be interpreted as the direct impact on hROS production at the ubiquinone binding site of complex II. The remaining hROS relative to inhibition control which was still detected in the presence of atpenin A5 might be produced (i) somewhere between Fp and Ip subunit of complex II or (ii) at complex III with electron flow from sources other than complex II. Antimycin A (5 μM), a Q_i site inhibitor of complex III, caused more decrease in hROS production compared to atpenin A5 treatment. If the hROS level detected by atpenin A5 treatment is still formed by complex II as in (i), comparable level of hROS should have been detected by antimycin A

treatment, since inhibition of complex III also cause inhibition of upstream processes including complex II, but in this experiment this was not observed (Fig. 14-B, C). In order to identify the alternative source of electrons driven hROS production in IR-mimicking condition as in (ii), the contribution of DHODH was evaluated by ferulenol (5 μM). Surprisingly, ferulenol decreased the hROS level in Panc-1 cells, but not to the same extent in HDF cells, indicating that the contribution of DHODH was specific to Panc-1 cells. In addition, hROS production was not reduced to the dimethyl malonate level by ferulenol treatment but to levels lower than atpenin A5 treatment. This result suggests that during IR-mimicking condition, in addition to complex II, DHODH directly fuels hROS production. This indicates that during IR-mimicking condition, dihydroorotate as well as succinate might accumulate and that hROS is produced by flow of electrons from DHODH and complex II, respectively. To support this hypothesis, treatment of pre-hypoxic cells with succinate at the concentrations determined during hypoxia (i.e., 38.2 and 16.9 μM, for Panc-1 and HDF, respectively) did not restore the hROS production to control levels (Fig. 15A), suggesting that in addition to succinate, another source of electrons may contribute to hROS production in IR-mimicking condition, which is most likely to be dihydroorotate. Because of high contribution of DHODH to hROS production, considerably fluorescence should have been detected in dimethyl malonate treated cells which was not the case. One possibility is that dimethyl malonate may inhibit both of complex II and DHODH. However, using purified human DHODH, 5 mM of dimethyl malonate as well as its demethylated

metabolite (malonate) showed no inhibition effect on the enzyme. It still remains unclear why 5 mM of dimethyl malonate potently inhibited hROS production in IR-mimicking condition. Remaining possibility such as the existence of another target molecule of dimethyl malonate contributing to hROS production is currently under investigation.

In HDF cells, neither atpenin A5 nor ferulenol inhibited hROS production, although dimethyl malonate significantly reduced hROS level. Treatment with antimycin A reduced hROS level but not to the same extent as dimethyl malonate. As for the Panc-1 cells, additional investigation is needed to solve the puzzle.

Both dimethyl malonate treatment and pH neutralization in HDF cells decreased hROS production in IR-mimicking condition.

In HDF cells, succinate did not accumulate in hypoxic period at pH 7.4 (Fig. 12). At pH 6.9, inhibition of complex II at its FAD site by dimethyl malonate significantly reduced hROS production, but not to the pre-hypoxic level (Fig. 15). At pH 7.4, addition of dimethyl malonate reduced hROS production to the pre-hypoxic level (Fig. 15). From the result that both dimethyl malonate treatment and pH neutralization completely abolished hROS production after IR-mimicking condition in HDF cells, it can be inferred that in IR injury dimethyl malonate treatment and pH neutralization have additive suppressive effect on hROS production (Fig. 15B). This suggests that it may be advantageous to treat the local tissue acidemia back to the normal pH, for example, by HCO_3^- as soon as possible after

reperfusion.

2-3.Discussion

Among hROS, hydroxyl radical plays the most important role in damaging cells. Previous studies of mitochondrial ROS production were performed using ROS markers such as dihydroethidium (DHE) (*156*) and MitoSOX, which have relatively higher specificity toward superoxide than other ROS. In this study the hROS production sites in mitochondrial ETC were evaluated using APF as one of the most specific indicators for hydroxyl radical and peroxynitrite (*157*), and revealed that under pH 6.9, complex II has the ability to produce hROS at high rate following IR-mimicking condition..

During cardiac ischemia, it is known that cytosolic pH decreases, due in part to increased lactate production via anaerobic glycolysis (*158*). However, no studies linking pH decrease and hROS production have been described. It has also been reported that succinate accumulates during cardiac ischemia and IR (*108, 109, 159*), although the correlation between succinate accumulation and hROS production as well as its production site(s) had still been unclear. In order to obtain deeper insights into the mechanism of hROS production, I investigated the effects of acidic pH on the rate of mitochondrial hROS production. I also analyzed the changes in concentration of accumulated succinate within the time course of IR-mimicking condition using substrates and inhibitors of ETC enzymes and found that hROS is mainly produced by complex II and that low pH (pH 6.9) augments the production of hROS compared to at physiological pH 7.4.

It is widely acknowledged that main sources of ROS production (mainly superoxide, $O_2^{\cdot -}$)

in mitochondria are complex I (*160*) and complex III (*161*) both of which comprise ETC in mitochondrial inner membrane. It has been reported that complex II contributes little to ROS production in mammalian mitochondria under normal oxygen conditions unless mutated (*162*). Mutated form of complex II was reported to produce ROS at high rates as observed in mitochondrial disease (*19*). In this study, I revealed that under pH 6.9 the wild-type complex II also has the ability to produce hROS at high rate following IR-mimicking condition.

Indeed, complex I can produce ROS under certain conditions (*163*), although its contribution to hROS production at least at 30 min following IR-mimicking treatment was proven to be negligible. However, strong contribution to hROS production by complex II was found, at least in Panc-1 and HDF cell lines. I also demonstrated that in addition to complex II, Panc-1 cells also produced hROS by the electron flow from DHODH, thus identifying a novel link between nucleotide metabolism and hROS production.

Our group have previously demonstrated that hypoxia induces cancer cells to express type II Fp of complex II which leads to its increased QFR activity (*17*) accounting for succinate accumulation during hypoxic period. For the mechanism of hROS production at FAD site of complex II, it was suggested that peroxynitrite-mediated oxidative modifications of complex II occurs (*112, 164*). In complex II, oxidative impairment and enhanced tyrosine nitration of the 70 kDa FAD-binding protein may occur in the post-ischemic myocardium and this process was linked to peroxynitrite *in vivo* (*110*). However, the source of

peroxynitrite remained elusive (*110*). In this study, I showed that accumulation of succinate during ischemia boosts hROS production during reperfusion by complex II somewhere between FAD and [Fe-S] redox centers, which might be the source of peroxynitrite causing tyrosine nitration observed *in vivo (165)*. I also showed that this hROS production can be prevented by treatment of complex II inhibitor binding at FAD-binding subunit providing a promising strategy to prevent IR injury. It is still not conclusive from this work whether or not if complex III is directly involved in hROS production, since inhibition of complex III can lead to accumulation of quinol and reverse flow of electrons through complex II where hROS is produced. In addition to succinate accumulation, I provide evidence that during IR-mimicking condition, dihydroorotate can also be accumulated and become a direct source of hROS or provide electrons to produce hROS via complex II. In some cancer cells living under 1% O_2/glc(-)gln(-) conditions, pyrimidine biosynthesis is totally dependent upon the *de novo* pathway (*120, 122, 123*), because aberrant proliferation demands high pyrimidine pool that cannot be supplied by the salvage pathway. This may be the reason why in Panc-1 cells substantial flow of electrons from DHODH results in hROS production. In HDF cells, treatment with ferulenol did not change significantly hROS production level, while dimethyl malonate strongly suppressed hROS production. These results indicate that in the case of HDF, during IR-mimicking condition, complex II is the major, if not, the only source of hROS production site while DHODH site being negligible.

From the findings that complex II inhibitor dimethyl malonate strongly suppressed

hROS production following IR-mimicking condition, dimethyl malonate was suggested as a potential therapeutic drug for IR injury. Also acidic condition at pH 6.9 promoted succinate production at complex II under hypoxia, followed by larger amount of hROS generation, suggesting that keeping the local pH of tissues at 7.4 may prevent hROS production after IR. The observations that hROS is generated at complex II and DHODH but not complex I and III will open possibilities to the development of inhibitors for treatment of injury caused by hROS during IR.

Conclusion

A novel cycling assay was developed for the determination of succinate concentration and was proven to be efficient, specific and reproducible. This assay can accurately detect succinate levels in the cell-cultured medium as well as intracellular extracts. In this study, by taking advantage of this new method, the ETC electron flow leading to succinate production in cancer as well as normal cells cultured under 21% O_2/glc(+)gln(+) and 1% O_2/glc(-)gln(-) conditions were evaluated. It is concluded that 1% O_2/glc(-)gln(-) conditions promote mitochondrial complex II to function as QFR producing succinate, which then facilitates cellular proliferation. In addition, the origin of electrons used by complex II to produce succinate under 1% O_2/glc(-)gln(-) conditions were identified as complex I and DHODH, revealing a novel link between nucleotide metabolism and fumarate respiration in cancer cells providing a promising candidate for drug development targeting tumour cells living under microenvironment.

By combining the novel succinate determination assay and specific detection of hROS by APF, I also investigated the involvement of succinate onto hROS production and provided a direct evidence that mitochondrial complex II and possibly DHODH are the responsible hROS production site at 30 min following IR-mimicking condition and complex I has little role in hROS production. Thus, complex II as well as DHODH has potential to be drug targets for the treatment of IR.

Figures and tables

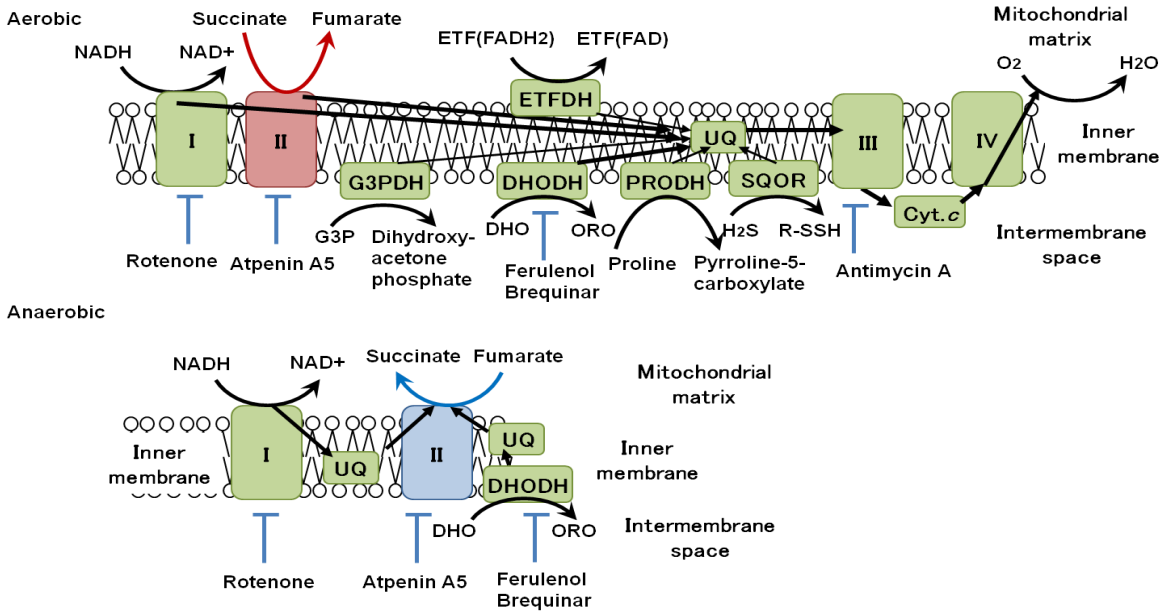

Figure 1

Schematic representation of electron transport chain during normoxia and hypoxia

In aerobic respiration, complex II catalyzes oxidation of succinate to form fumarate as succinate–ubiquinone reductase (SQR), and electrons produced in this process are transferred to complex III, IV in these orders. In addition to complex I and II, there are several peripheral respiratory enzymes shuttling electrons to the ubiquinone (UQ) pool in ETC: dihydroorotate dehydrogenase (DHODH), glycerol-3-phosphate dehydrogenase (G3PDH), proline dehydrogenase (PRODH), sulfide:quinone oxidoreductase (SQOR) and electron-transfer flavoprotein dehydrogenase (ETFDH). In anaerobic respiration, on the other hand, quinol-fumarate reductase (QFR) activity of complex II to form succinate from fumarate increases, and thus complex II accepts electrons from other complexes. This "fumarate respiration" functions in the cancer cells, which is mainly composed of complex I and QFR activity of complex II. In fumarate respiration, menaquinol (MKH_2) is supposed to work as electron receptor.

A

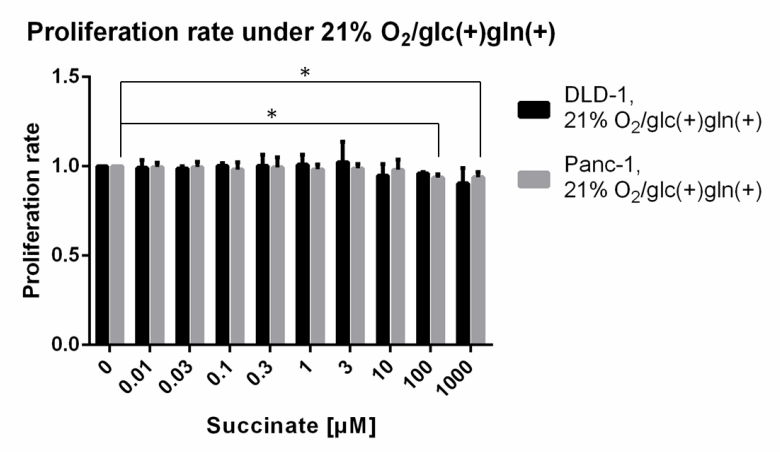

B

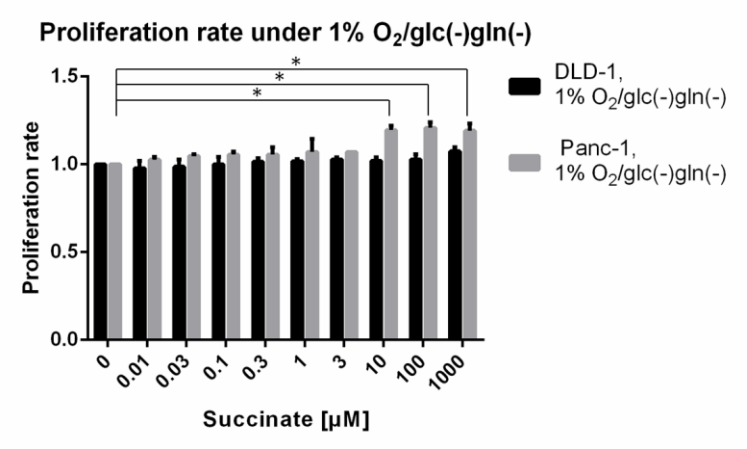

Figure 2

Effect of succinate accumulation on cell proliferation rate under normoxia and hypoxia

Proliferation rate of DLD-1 and Panc-1 cells were determined under 21% O_2/glc(+)gln(+) (A) and 1% O_2/glc(-)gln(-) conditions (B) in the presence of different concentrations of succinate (see material and methods for detail). Statistical analyses were performed using Student's t test. Values of $p < 0.05$ were considered statistically significant, and * means $p < 0.05$.

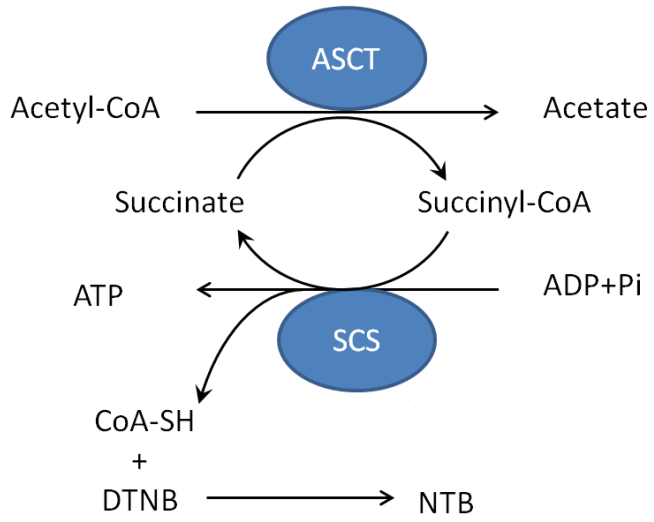

Figure 3

ASCT/SCS succinate cycling assay

Succinate concentration was assayed using purified recombinant ASCT from *Trypanosoma brucei* and SCS from a prokaryote. ASCT produces succinyl-CoA from acetyl-CoA and succinate. Next, SCS converts succinyl-CoA into CoA and succinate. In this reaction, a molecule of ATP is also generated. The thiol group of CoA reduces DTNB to NTB which can be measured by the increase in absorbance at 412 nm.

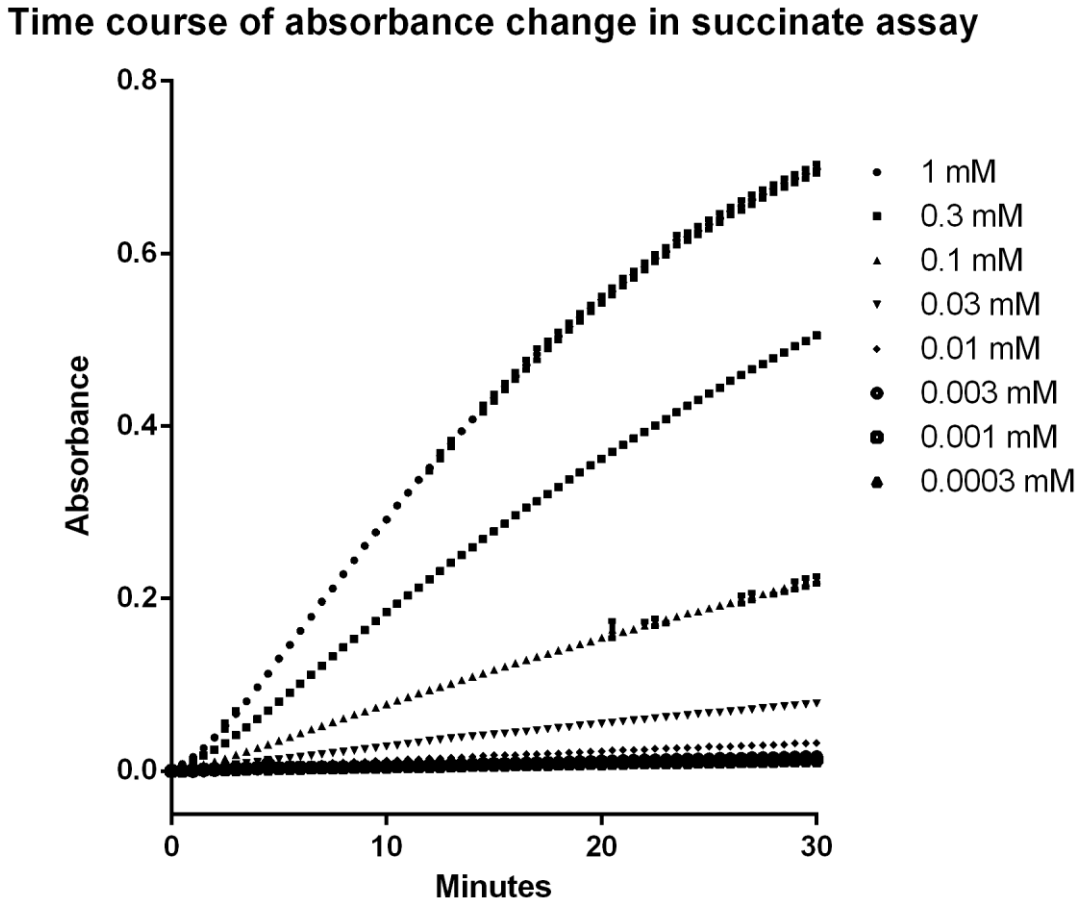

Figure 4

Time course of absorbance rate in ASCT/SCS succinate cycling assay

The graph shows the time course of ASCT/SCS succinate cycling assay for each succinate concentration using 250 ng/mL of ASCT. In the ASCT/SCS succinate cycling assay, the absorbance change at 412 nm were recorded at the interval of 30 seconds for 30 minutes. The slope was calculated by dividing the change in absorbance between 3.5 min and 10 min for each graph obtained from different concentrations of succinate.

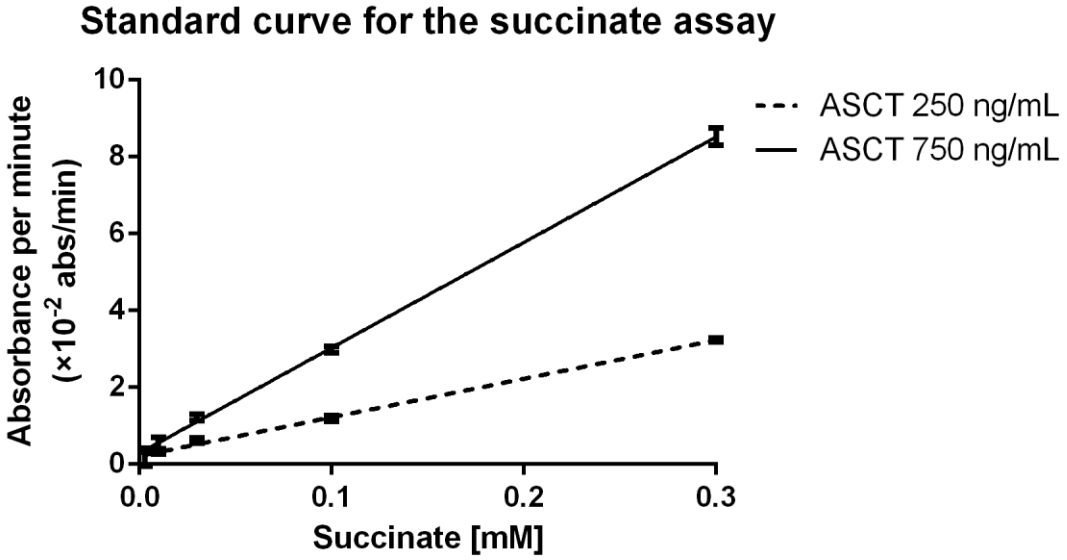

Figure 5

The standard curve for the succinate assay

In the ASCT/SCS succinate cycling assay, a linear correlation was observed between succinate concentration and the absorbance slope between 3.5 min and 10 min in the absorbance graph (Fig. 4). Results are for 250 and 750 ng/mL of ASCT, respectively. At the concentration of 250 and 750 ng/mL of ASCT and 1.1 U/mL of SCS, the correlation coefficient was $R^2 = 0.9974$ and 0.9997, respectively, and the minimum limit of determination of succinate was 0.01 mM ($p < 0.0001$) in both ASCT concentrations tested. Results are means ± S.D. for at least three independent experiments.

A-1

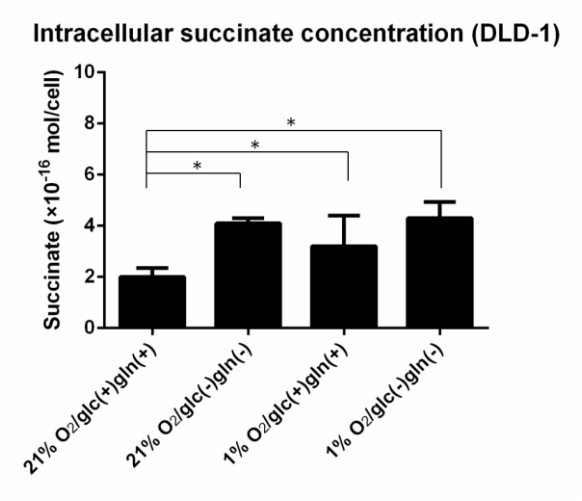

B-1

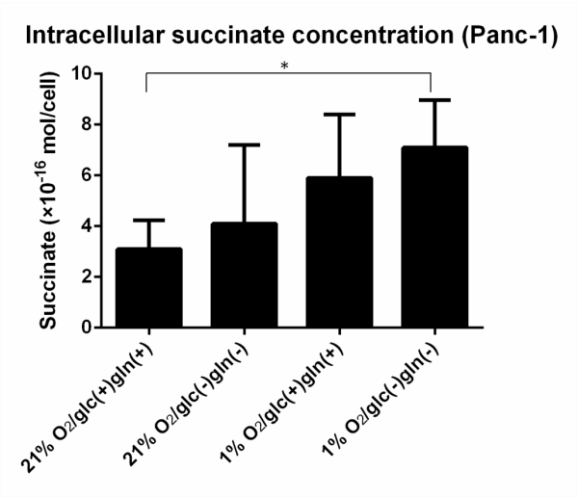

A-2

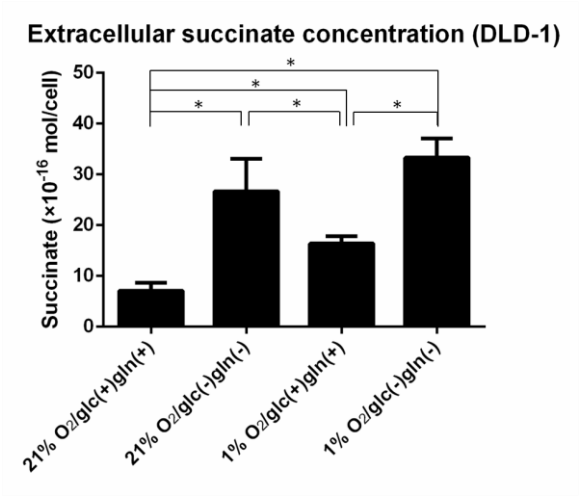

B-2

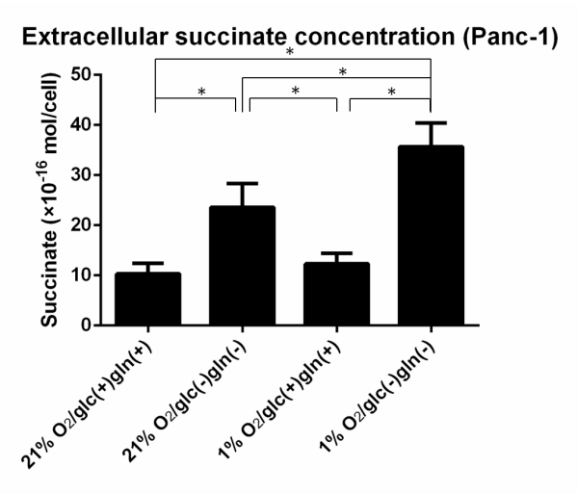

Figure 6

Intra- and extracellular amount of succinate per cell

DLD-1 cells and Panc-1 cells were seeded at 1.0×10^5/mL in 96-well plates under 21% O_2 or 1% O_2 and glc(+)gln(+) or glc(-)gln(-) conditions. After incubation for 24 hr at 37°C, intra- and extracellular succinate concentration was measured by ASCT/SCS succinate cycling assay. Intracellular and extracellular succinate amount was normalized by the number of the cells. Panel A-1, A-2, B-1 and B-2 shows the intracellular succinate concentration of DLD-1, extracellular succinate concentration of DLD-1, intracellular succinate concentration of Panc-1 and extracellular succinate concentration of Panc-1, respectively. Statistical analyses were performed using Student's t test. Values of $p < 0.05$ were considered statistically significant, and * means $p < 0.05$.

A

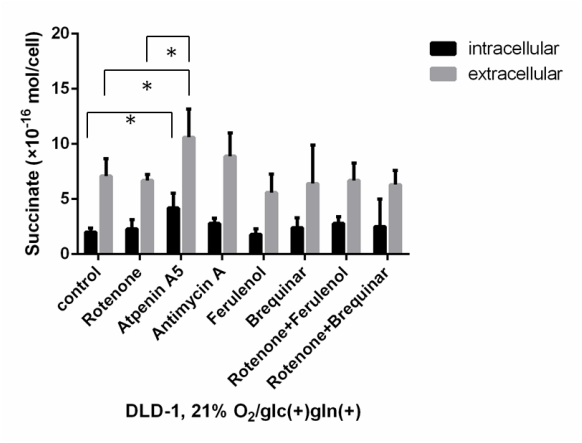
Succinate (×10-16 mol/cell)
intracellular
extracellular
control
Rotenone
Atpenin A5
Antimycin A
Ferulenol
Brequinar
Rotenone+Ferulenol
Rotenone+Brequinar
DLD-1, 21% O2/glc(+)gln(+)

B

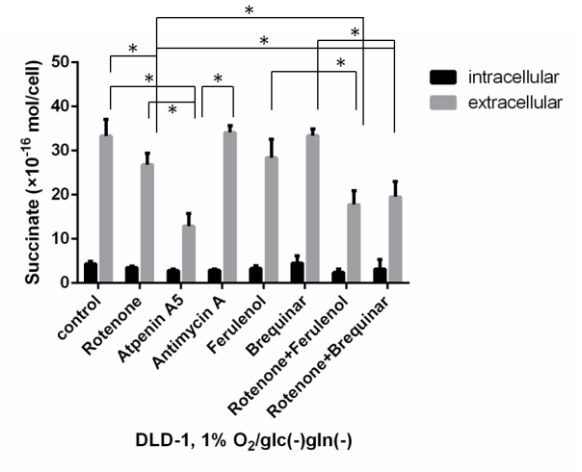
Succinate (×10-16 mol/cell)
intracellular
extracellular
control
Rotenone
Atpenin A5
Antimycin A
Ferulenol
Brequinar
Rotenone+Ferulenol
Rotenone+Brequinar
DLD-1, 1% O2/glc(-)gln(-)

C

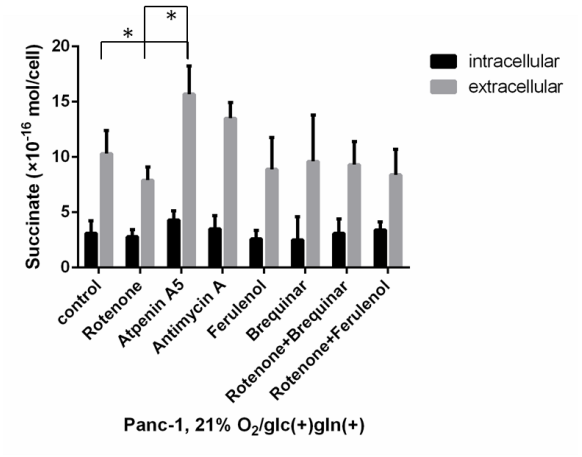
Succinate (×10-16 mol/cell)
intracellular
extracellular
control
Rotenone
Atpenin A5
Antimycin A
Ferulenol
Brequinar
Rotenone+Brequinar
Rotenone+Ferulenol
Panc-1, 21% O2/glc(+)gln(+)

D

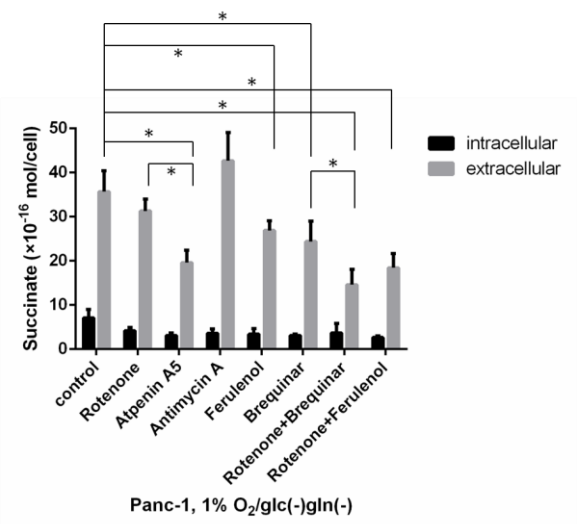
Succinate (×10-16 mol/cell)
intracellular
extracellular
control
Rotenone
Atpenin A5
Antimycin A
Ferulenol
Brequinar
Rotenone+Brequinar
Rotenone+Ferulenol
Panc-1, 1% O2/glc(-)gln(-)

E

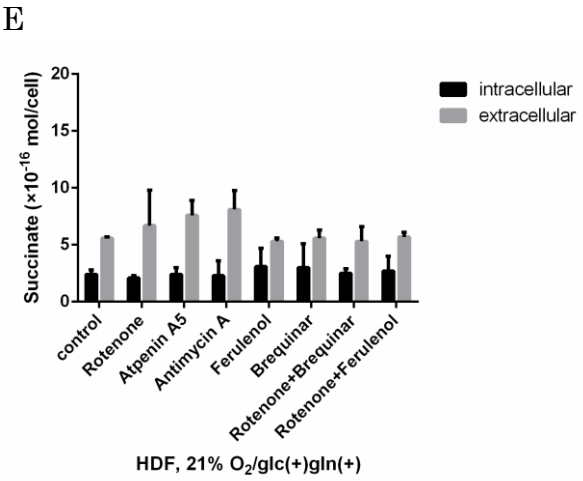
Succinate (×10-16 mol/cell)
intracellular
extracellular
control
Rotenone
Atpenin A5
Antimycin A
Ferulenol
Brequinar
Rotenone+Brequinar
Rotenone+Ferulenol
HDF, 21% O2/glc(+)gln(+)

F

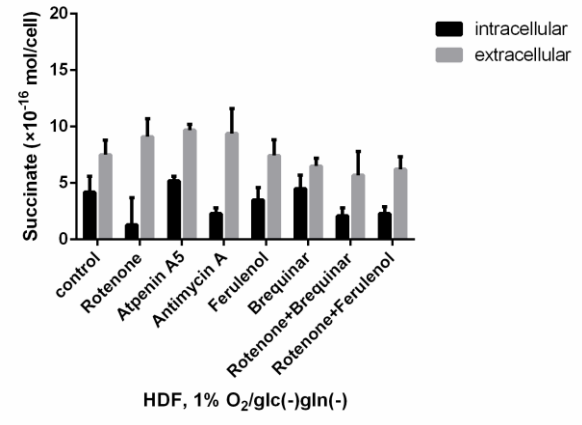
Succinate (×10-16 mol/cell)
intracellular
extracellular
control
Rotenone
Atpenin A5
Antimycin A
Ferulenol
Brequinar
Rotenone+Brequinar
Rotenone+Ferulenol
HDF, 1% O2/glc(-)gln(-)

Figure 7

Effects of ETC inhibitors on succinate concentration

The level of intra- and extracellular succinate in 21% O_2/glc(+)gln(+) and 1% O_2/glc(-)gln(-) conditions was measured with each ETC inhibitor added in the medium and normalized by the number of the cells. Panel A/B, C/D, and E/F show the results of DLD-1 cells, Panc-1 cells, and HDF cells, respectively. Panel A/C/E and B/D/F show the results of 21% O_2/glc(+)gln(+) and 1% O_2/glc(-)gln(-) conditions. Statistical analyses were performed using Student's t test. Values of $p < 0.05$ were considered statistically significant, and * means $p < 0.05$.

A

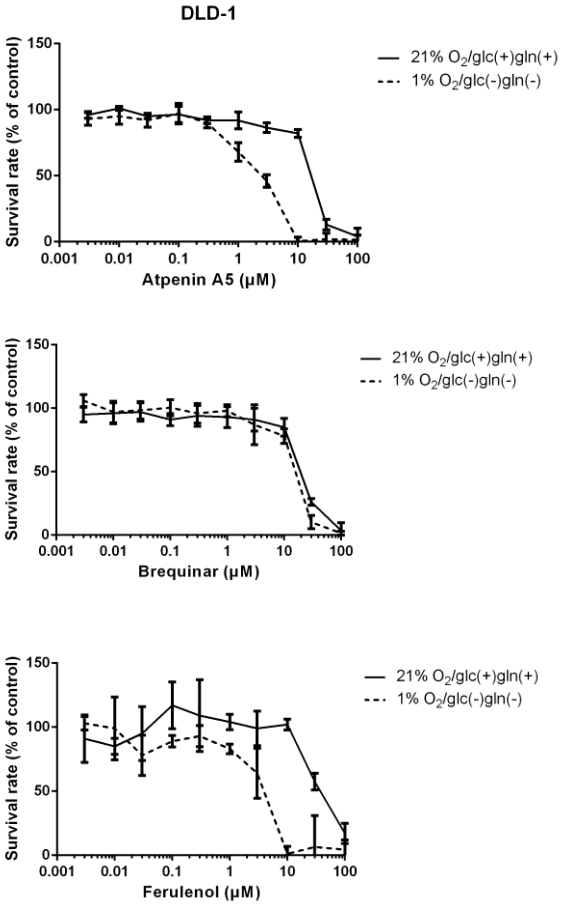
DLD-1
Survival rate (% of control)
150
100
50
0
0.001
0.01
0.1
1
10
100
Atpenin A5 (μM)
21% O2/glc(+)gln(+)
1% O2/glc(-)gln(-)
Brequinar (μM)
Ferulenol (μM)

B

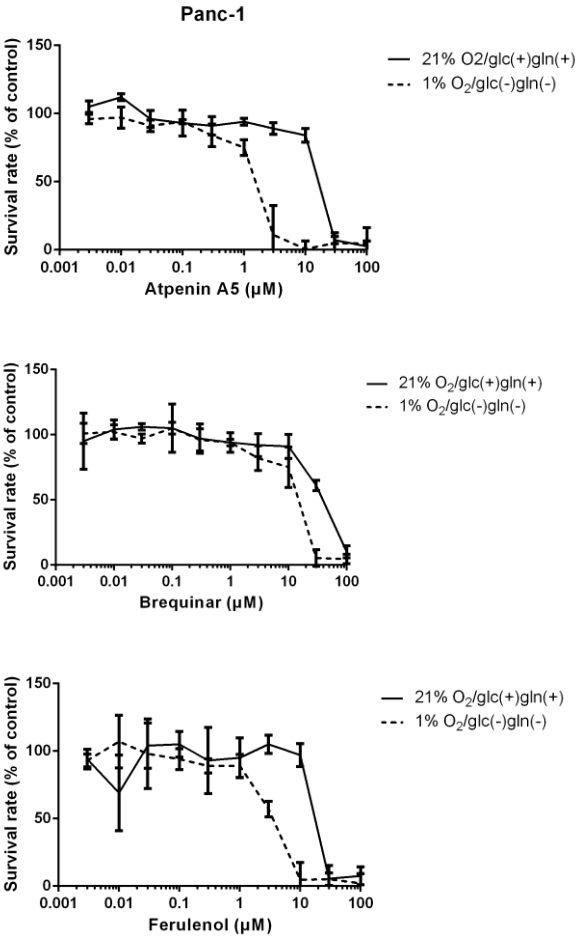
Panc-1
Survival rate (% of control)
150
100
50
0
0.001
0.01
0.1
1
10
100
21% O2/glc(+)gln(+)
1% O2/glc(-)gln(-)
Atpenin A5 (μM)
Brequinar (μM)
Ferulenol (μM)

C

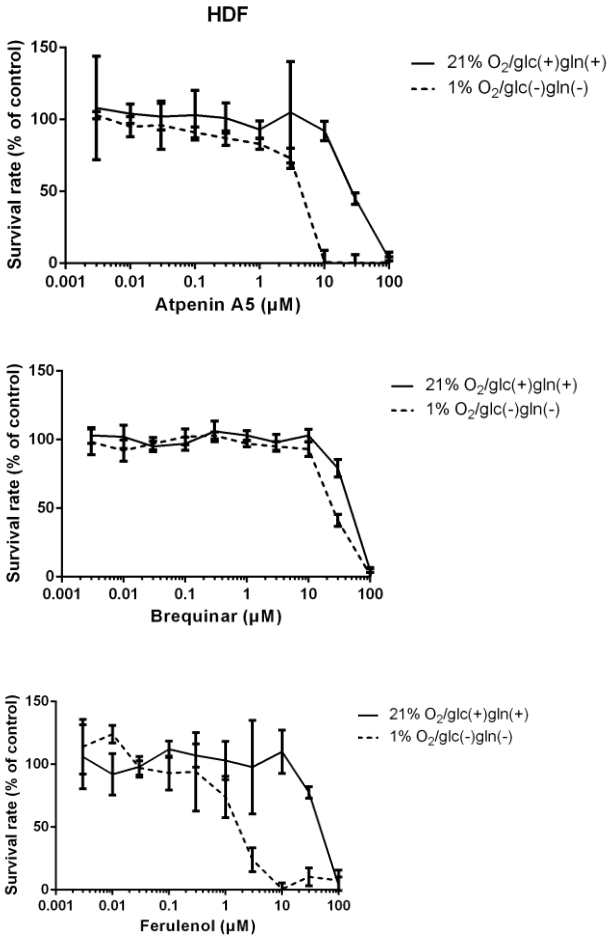

Figure 8

Anti-survival effect of DHODH inhibitors and atpenin A5 on Panc-1, DLD-1, and HDF cells

The graph shows the anti-proliferative effect of DHODH inhibitors (ferulenol and brequinar) and atpenin A5 in 21% O_2/glc(+)gln(+) and 1% O_2/glc(-)gln(-) conditions. The cell viability was evaluated by counting cell numbers. The relative proliferation rate was calculated by dividing the cell number of the well of interest by that of the well untreated. Panel A, B and C represent the survival rate (% of control) of DLD-1, Panc-1 and HDF, respectively.

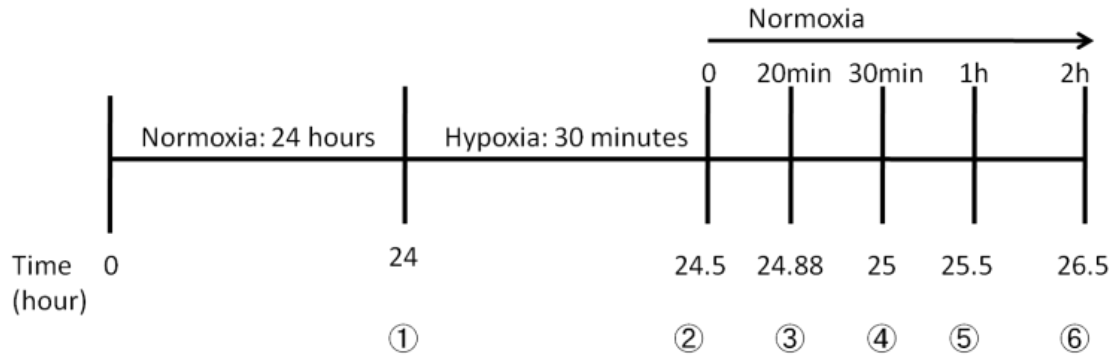

Figure 9

Protocol of investigating the time course of hROS production and succinate level in IR-mimicking condition

The cells were exposed to 30 min of hypoxia and various durations (20 min, 30 min, 1 h and 2 h) of normoxia. At each time point, the cells were examined for hROS with APF staining and assayed for succinate level using ASCT/SCS succinate cycling assay.

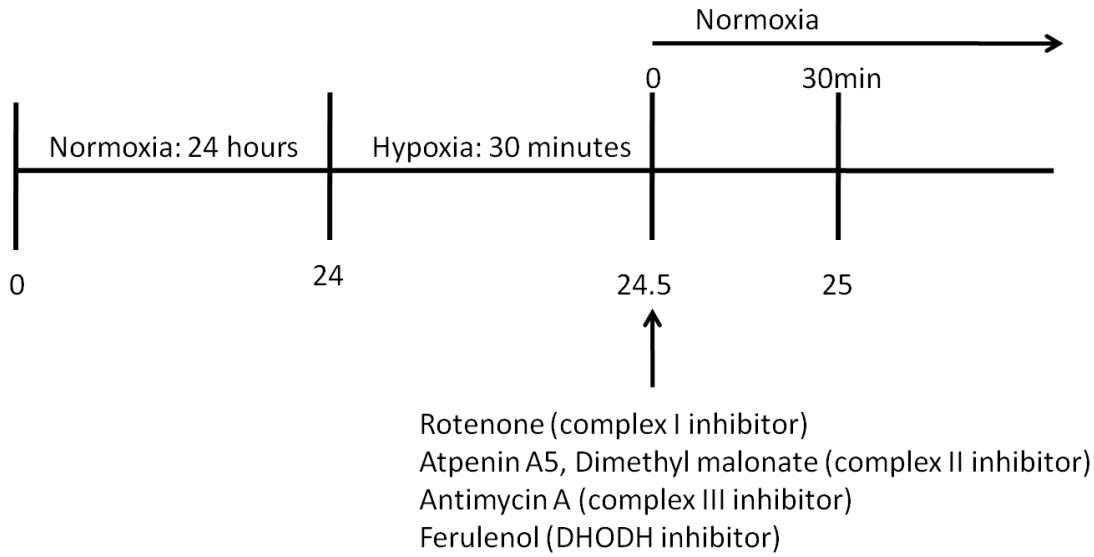

Figure 10

Protocol of investigating the effect of mitochondrial ETC inhibitors on hROS production and succinate level

The cells were treated with each ETC inhibitor following 30 min of ischemia and then underwent 30 min of normoxia. The cells were examined for hROS with APF staining and assayed for succinate level using ASCT/SCS succinate cycling assay.

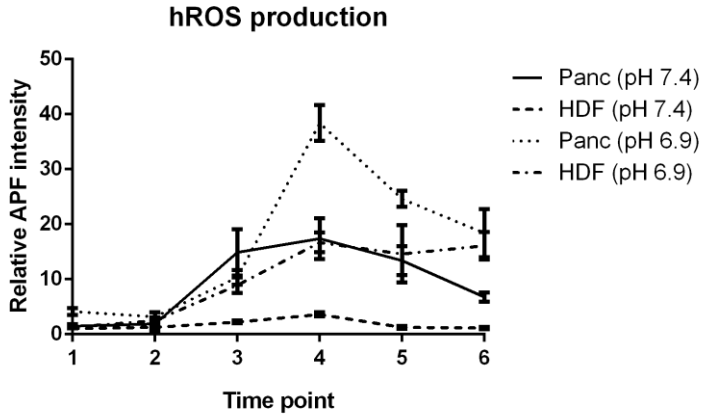

Figure 11

Time course of hROS production in IR-mimicking condition

To investigate the time course of hROS production, the hROS level in Panc-1 and HDF cells was measured by APF during and after hypoxic period at pH 7.4 or 6.9. The graph shows the APF intensity relative to time point of ① of HDF under pH 7.4.

A

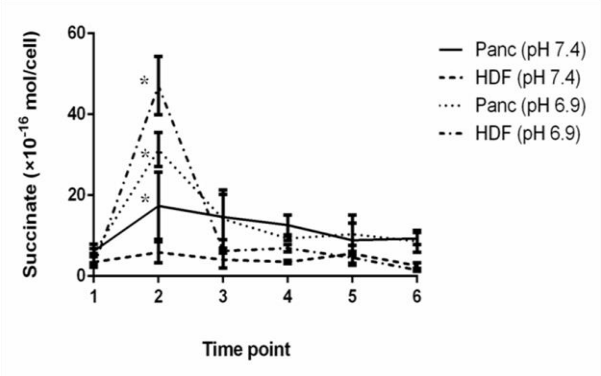

B

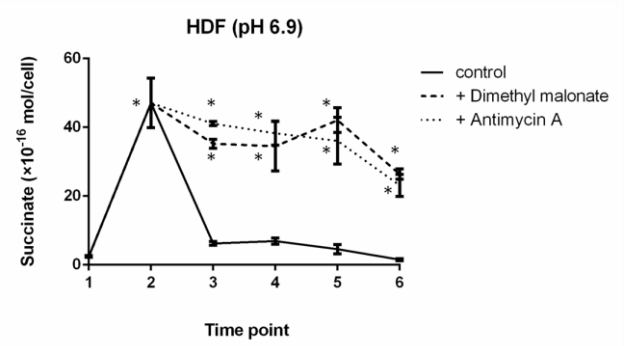

C

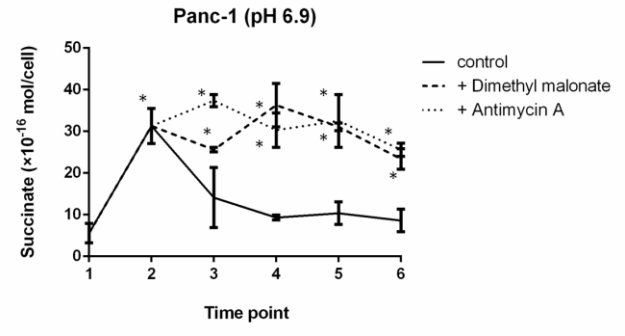

Figure 12

Succinate level during and after IR-mimicking treatment

Extracellular succinate level per cell during and after IR-mimicking treatment was examined by the succinate cycling assay. The numbers of time course correspond to those in Fig. 9. Panel A shows extracellular succinate level at pH 7.4 and 6.9. Panel B shows extracellular succinate level in HDF at pH 6.9 with dimethyl malonate or antimycin A added at the end of hypoxic period. Panel C shows extracellular succinate level in Panc-1 at pH 6.9 with dimethyl malonate or antimycin A added at the end of hypoxic period. The controls in panel B and C show the identical results with HDF (pH6.9) and Panc-1 (pH6.9) in panel A, respectively. Statistical analyses were performed using Student's t test. Values of $p < 0.05$ were considered statistically significant, and * means $p < 0.05$ (compared to time point 1).

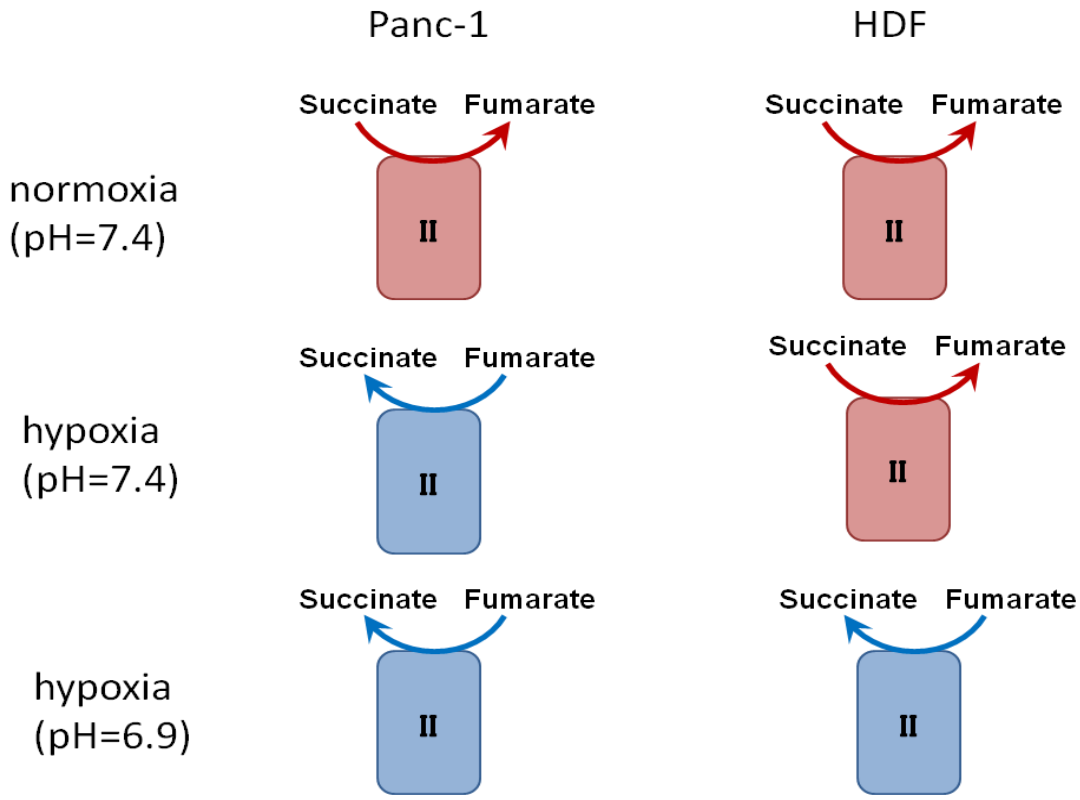

Figure 13

Proposed schema of enzymatic activity of complex II

This figure illustrates the proposed schema of enzymatic activity of complex II. In normoxia, complex II acts as SQR catalyzing the oxidation of succinate to form fumarate. In HDF, both hypoxia and acidic condition (pH = 6.9) are the essential elements for complex II to work as QFR to produce succinate, although in Panc-1 cells hypoxia alone can induce succinate production.

A　HDF pH7.4

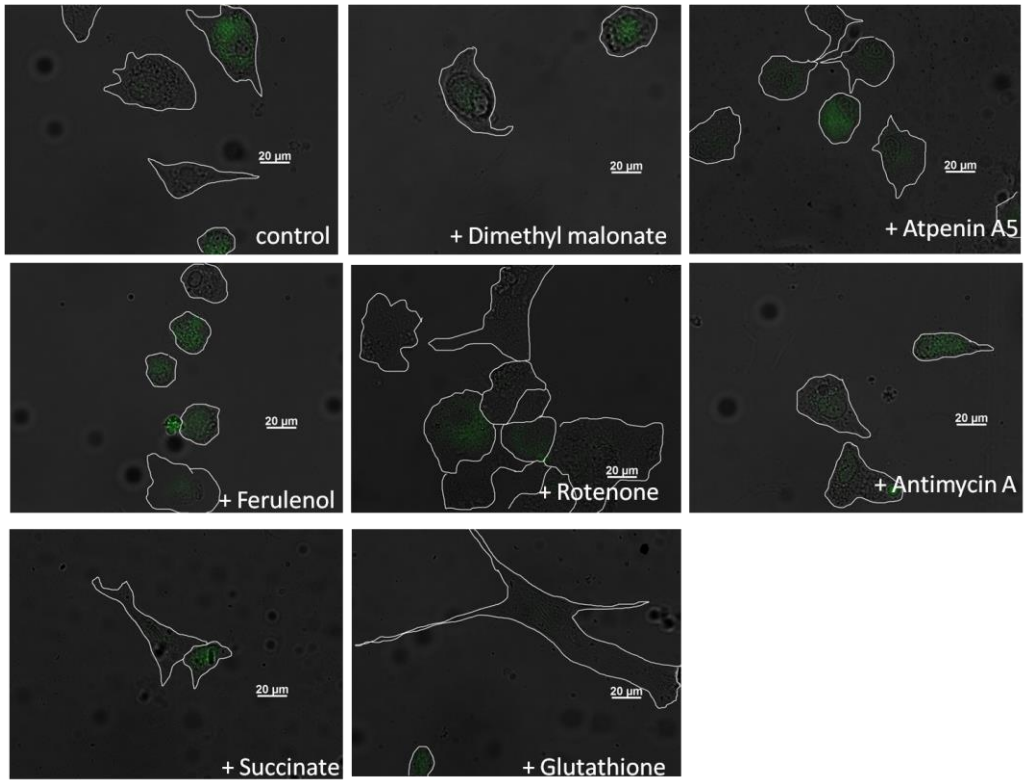

B　Panc-1 pH7.4

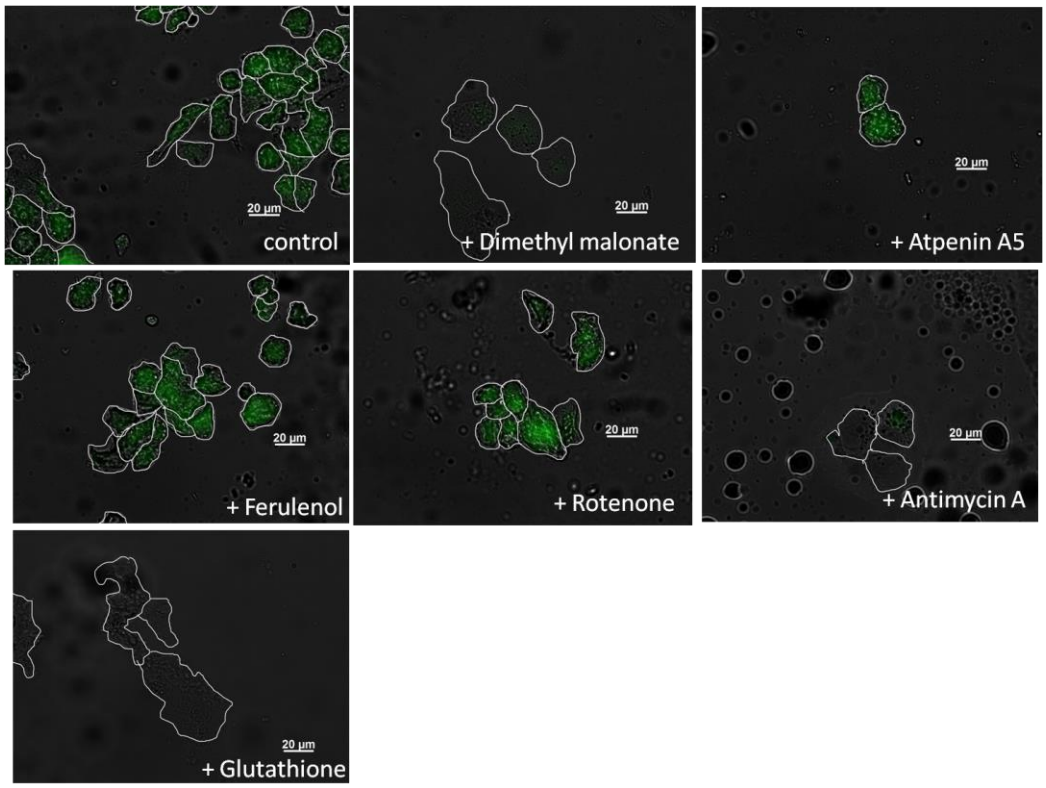

C　HDF pH6.9

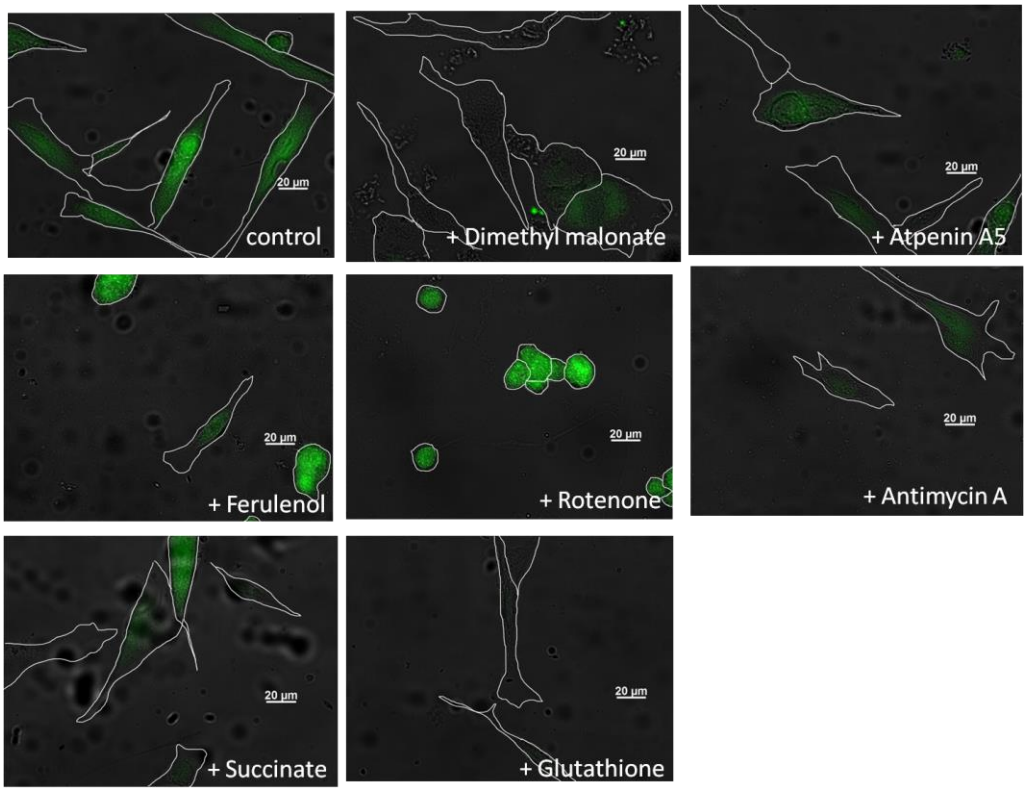

D　Panc-1 pH6.9

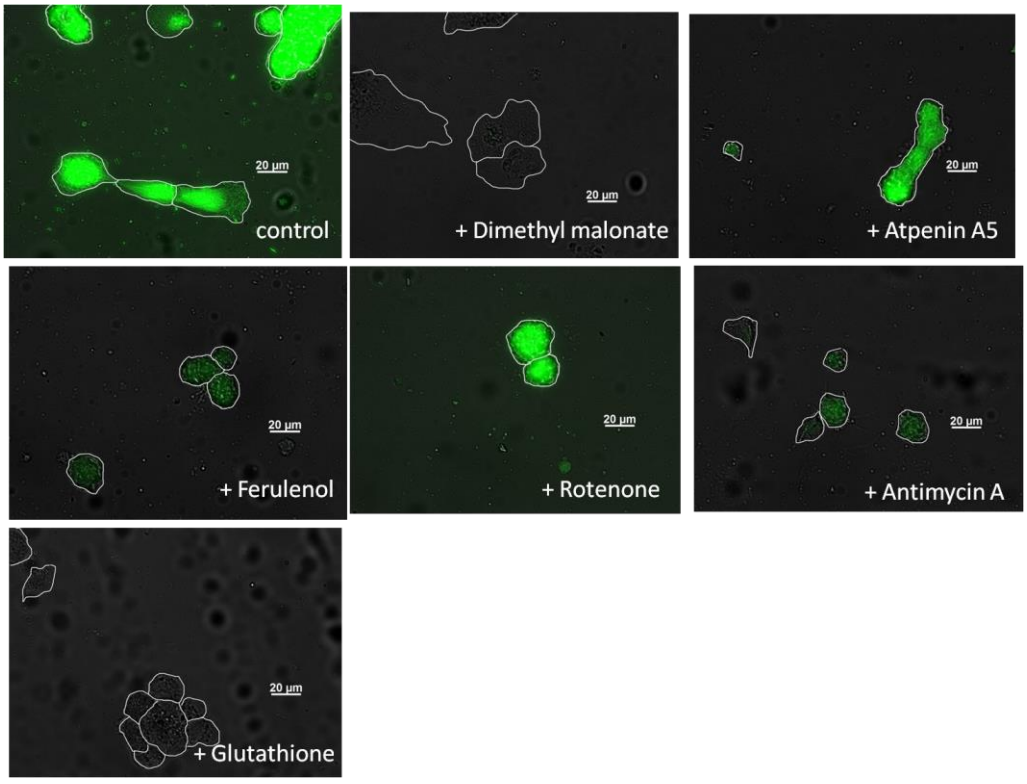

Figure 14

Effects of mitochondrial complex inhibitors on IR-mimicking-treatment-induced hROS production.

The graph shows intracellular hROS level from cells cultured in the presence of ETC inhibitors. Fluorescence level of Aminophenyl Fluorescein (APF) was analysed by microscope for hROS level at the time point of ④ in Fig. 9, *i.e.*, after 30 min normoxia following hypoxia. Dimethyl malonate (5 mM), atpenin A5 (5 μM), ferulenol (5 μM), rotenone (5 μM), antimycin A (5 μM), succinate, and glutathione (10 mM) were added after 30 min exposure to hypoxia. Succinate was added at the concentration of 38.2 μM (Panc-1) and 16.9 μM (HDF), respectively. Panel A/C and B/D show representative images of HDF and Panc-1 cells, respectively. Panel A/B and C/D show the result under pH 7.4 and 6.9, respectively.

A

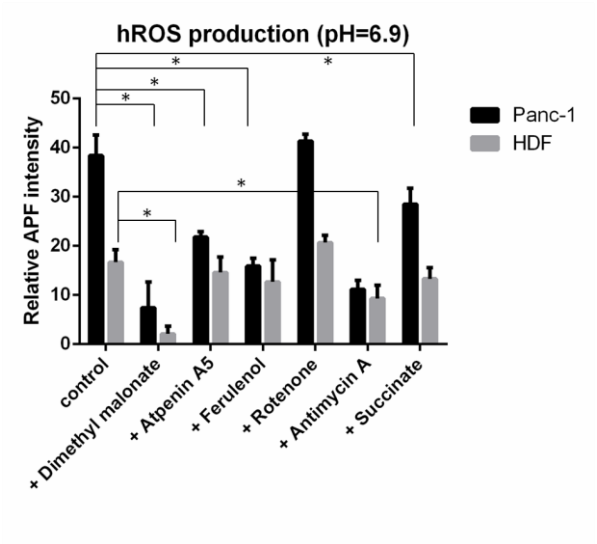

B

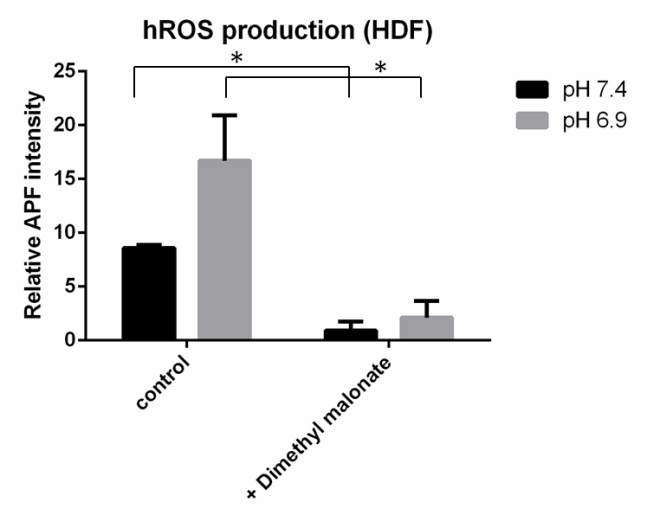

Figure 15

Quantitative analysis of hROS production level

Effects of mitochondrial ETC inhibitors on relative hROS production rates in Panc-1 cells and HDF cells were examined at the time point of ④ in Fig. 9, *i.e.*, after 30-min normoxia following hypoxia (**A**). **B** shows hROS production amount in HDF cells; the effects of pH (pH 6.9 and 7.4) and dimethyl malonate on hROS production were analyzed. The graph shows the APF intensity relative to time point of ① of HDF under pH 7.4. Dimethyl malonate (5 mM), atpenin A5 (5 μM), ferulenol (5 μM), rotenone (5 μM), antimycin A (5 μM), succinate, and glutathione (10 mM) were added after 30-min exposure to hypoxia. Succinate was added at the concentration of 38.2 μM (Panc-1) and 16.9 μM (HDF), respectively. Values are means ± SD of 60 cells observed in three independent experiments. Statistical analyses were performed using Student's t test. Values of $p < 0.05$ were considered statistically significant, and * means $p < 0.05$.

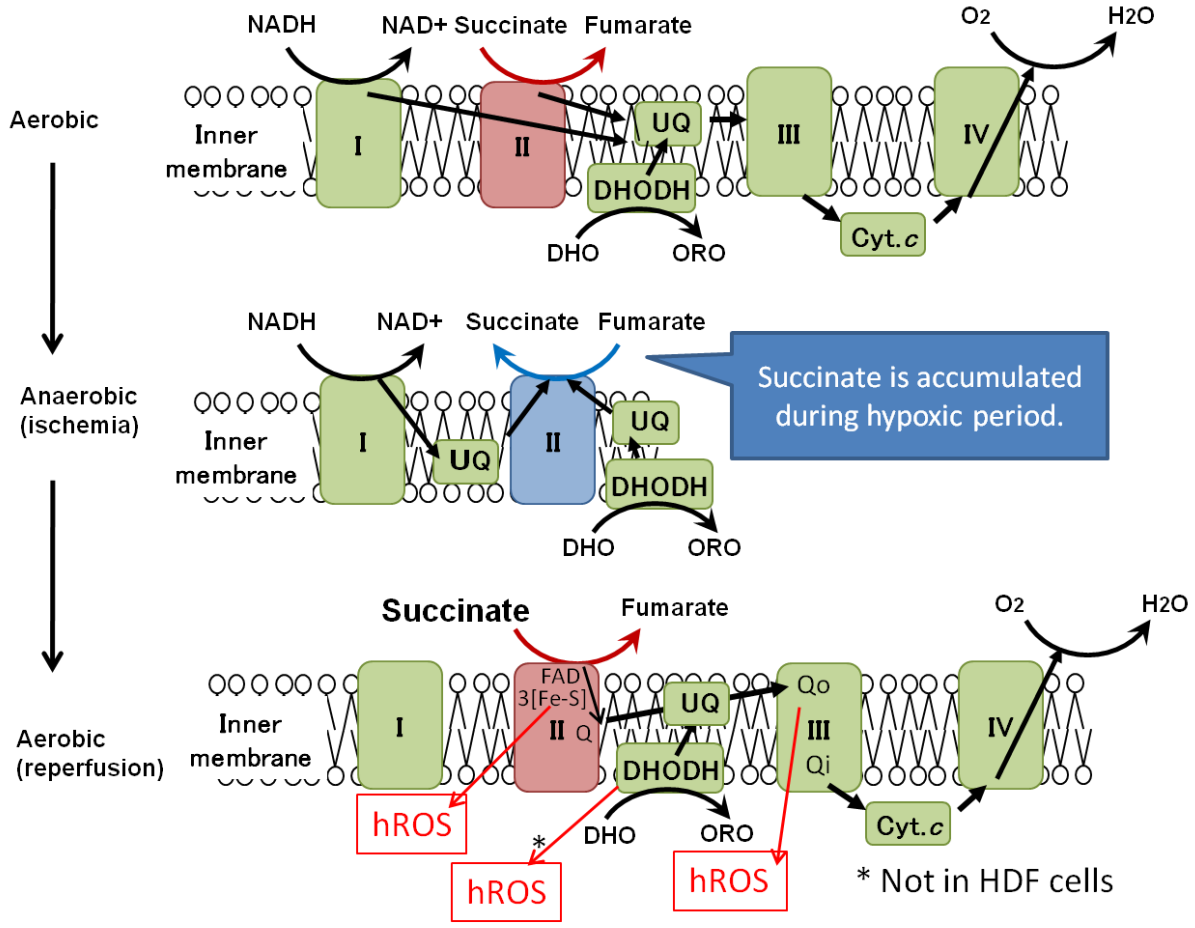

Figure 16

Putative electron flow in IR-mimicking-condition

Putative electron flow during aerobic repiration, ischemia and reperfusion-mimicking conditions are shown. In Panc-1 and HDF cells, ischemia-mimicking condition induces succinate accumulation which results in the electron flow from complex I to II as well as from DHODH to complex II. During reperfusion-mimicking condition, hROS may be generated by electrons flowing from complex II to III and IV at complex II (somewhere between Fp and Ip subunits), *Qo* site of complex III and DHODH. However, in HDF, hROS production by DHODH is negligible.

Appendix

The chemical structures of mitochondrial complex inhibitors (rotenone, atpenin A5, antimycin A, brequinar, ferulenol and A771726) are shown here.

Rotenone

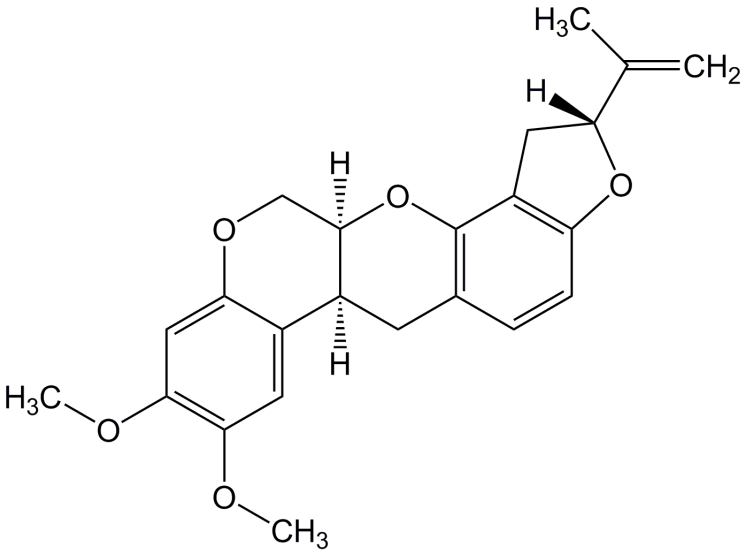

Atpenin A5

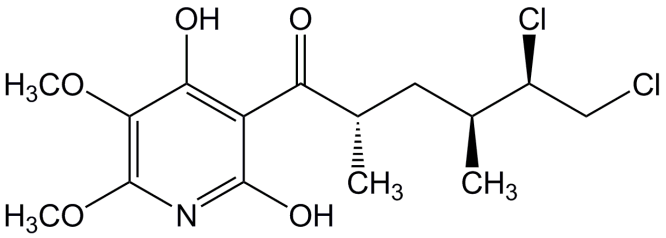

Antimycin A

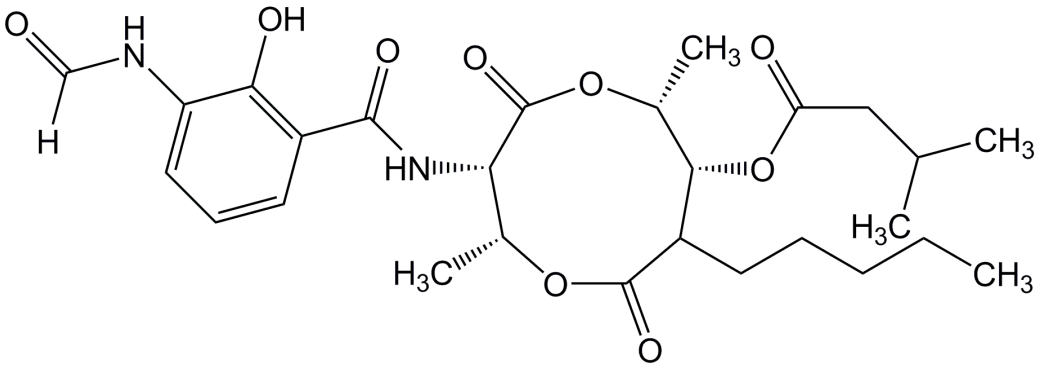

Brequinar

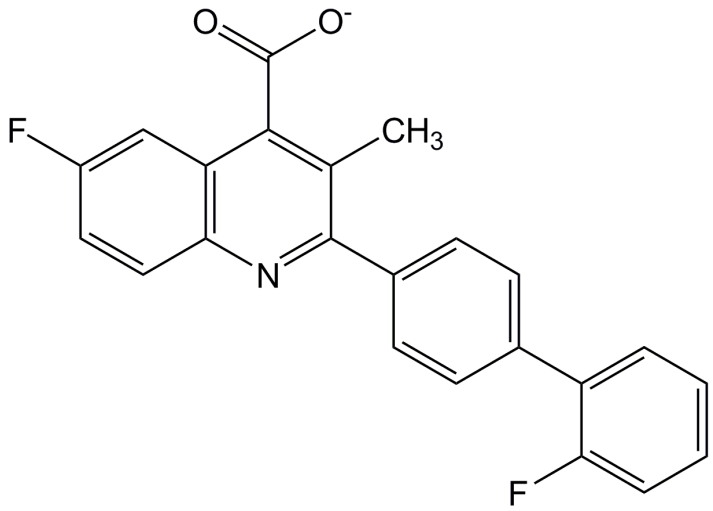

Ferulenol

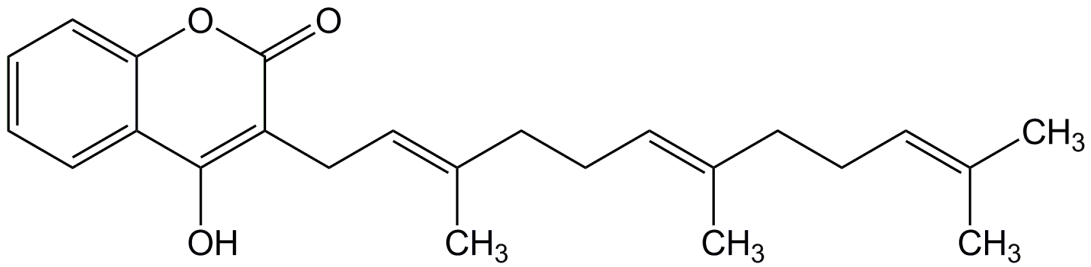

A771726

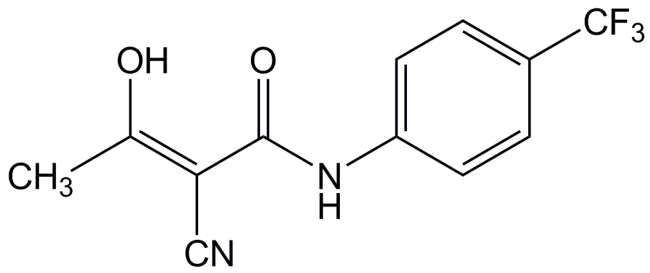

Acknowledgement

I am sincerely grateful to Professor Kiyoshi Kita for his professional guidance, continuous encouragement and unforgettable support. I would like to express my sincere gratitude to Dr. D. K. Inaoka and all the staffs at Department of Biomedical Chemistry.

Reference

1. G. S. Shadel, T. L. Horvath, Mitochondrial ROS Signaling in Organismal Homeostasis. *Cell* **163**, 560-569 (2015); published online EpubOct 22 (10.1016/j.cell.2015.10.001).
2. Fatty acid synthesis and mitochondrial localization. *Osterreichische Schwesternzeitung* **23**, 106-108 (1970); published online EpubApr (
3. G. P. Holloway, A. Bonen, L. L. Spriet, Regulation of skeletal muscle mitochondrial fatty acid metabolism in lean and obese individuals. *The American journal of clinical nutrition* **89**, 455S-462S (2009); published online EpubJan (10.3945/ajcn.2008.26717B).
4. W. Knecht, M. Loffler, Species-related inhibition of human and rat dihydroorotate dehydrogenase by immunosuppressive isoxazol and cinchoninic acid derivatives. *Biochemical pharmacology* **56**, 1259-1264 (1998); published online EpubNov 1
5. W. Seubert, [Mitochondrial fatty acid synthesis and pathologic formation of ketone bodies]. *Die Naturwissenschaften* **57**, 443-449 (1970); published online EpubSep
6. C. Moffat, L. Bhatia, T. Nguyen, P. Lynch, M. Wang, D. Wang, O. R. Ilkayeva, X. Han, M. D. Hirschey, S. M. Claypool, E. L. Seifert, Acyl-CoA thioesterase-2 facilitates mitochondrial fatty acid oxidation in the liver. *Journal of lipid research* **55**, 2458-2470 (2014); published online EpubDec (10.1194/jlr.M046961).
7. K. Zarse, S. Schmeisser, M. Groth, S. Priebe, G. Beuster, D. Kuhlow, R. Guthke, M. Platzer, C. R. Kahn, M. Ristow, Impaired insulin/IGF1 signaling extends life span by promoting mitochondrial L-proline catabolism to induce a transient ROS signal. *Cell metabolism* **15**, 451-465 (2012); published online EpubApr 4 (10.1016/j.cmet.2012.02.013).
8. S. Kosel, G. Hofhaus, A. Maassen, P. Vieregge, M. B. Graeber, Role of mitochondria in Parkinson disease. *Biological chemistry* **380**, 865-870 (1999); published online EpubJul-Aug (10.1515/BC.1999.106).
9. M. M. Muqit, S. Gandhi, N. W. Wood, Mitochondria in Parkinson disease: back in fashion with a little help from genetics. *Archives of neurology* **63**, 649-654 (2006); published online EpubMay (10.1001/archneur.63.5.649).
10. M. Wajner, A. U. Amaral, Mitochondrial dysfunction in fatty acid oxidation disorders: insights from human and animal studies. *Bioscience reports*, (2015); published online EpubNov 20 (10.1042/BSR20150240).
11. T. Bourgeron, D. Chretien, J. Poggi-Bach, S. Doonan, D. Rabier, P. Letouze, A. Munnich, A. Rotig, P. Landrieu, P. Rustin, Mutation of the fumarase gene in two siblings with progressive encephalopathy and fumarase deficiency. *The Journal of clinical investigation* **93**, 2514-2518 (1994); published online EpubJun (10.1172/JCI117261).

12. V. R. Biegen, J. P. McCue, T. A. Donovan, G. D. Shelton, Metabolic Encephalopathy and Lipid Storage Myopathy Associated with a Presumptive Mitochondrial Fatty Acid Oxidation Defect in a Dog. *Frontiers in veterinary science* **2**, 64 (2015)10.3389/fvets.2015.00064).
13. B. B. Ordys, S. Launay, R. F. Deighton, J. McCulloch, I. R. Whittle, The role of mitochondria in glioma pathophysiology. *Molecular neurobiology* **42**, 64-75 (2010); published online EpubAug (10.1007/s12035-010-8133-5).
14. B. E. Baysal, J. E. Willett-Brozick, E. C. Lawrence, C. M. Drovdlic, S. A. Savul, D. R. McLeod, H. A. Yee, D. E. Brackmann, W. H. Slattery, 3rd, E. N. Myers, R. E. Ferrell, W. S. Rubinstein, Prevalence of SDHB, SDHC, and SDHD germline mutations in clinic patients with head and neck paragangliomas. *Journal of medical genetics* **39**, 178-183 (2002); published online EpubMar
15. Q. Chen, A. K. Camara, D. F. Stowe, C. L. Hoppel, E. J. Lesnefsky, Modulation of electron transport protects cardiac mitochondria and decreases myocardial injury during ischemia and reperfusion. *American journal of physiology. Cell physiology* **292**, C137-147 (2007); published online EpubJan (10.1152/ajpcell.00270.2006).
16. G. Petrosillo, F. M. Ruggiero, N. Di Venosa, G. Paradies, Decreased complex III activity in mitochondria isolated from rat heart subjected to ischemia and reperfusion: role of reactive oxygen species and cardiolipin. *FASEB journal : official publication of the Federation of American Societies for Experimental Biology* **17**, 714-716 (2003); published online EpubApr (10.1096/fj.02-0729fje).
17. C. Sakai, E. Tomitsuka, M. Miyagishi, S. Harada, K. Kita, Type II Fp of human mitochondrial respiratory complex II and its role in adaptation to hypoxia and nutrition-deprived conditions. *Mitochondrion* **13**, 602-609 (2013); published online EpubNov (10.1016/j.mito.2013.08.009).
18. L. Nante, [Modifications induced by ischemia on the respiratory, succinic oxidase and amino acid oxidase activity of homogenates of volunatry muscle and on the succinic oxidase and adenosinetriphosphatase activity of the corresponding mitochondria]. *Lo sperimentale* **110**, 8-20 (1960); published online EpubJan-Feb (
19. B. A. Ackrell, Cytopathies involving mitochondrial complex II. *Molecular aspects of medicine* **23**, 369-384 (2002); published online EpubOct
20. H. Amino, A. Osanai, H. Miyadera, N. Shinjyo, E. Tomitsuka, H. Taka, R. Mineki, K. Murayama, S. Takamiya, T. Aoki, H. Miyoshi, K. Sakamoto, S. Kojima, K. Kita, Isolation and characterization of the stage-specific cytochrome b small subunit (CybS) of Ascaris suum complex II from the aerobic respiratory chain of larval mitochondria. *Molecular and biochemical parasitology* **128**, 175-186 (2003); published online EpubMay
21. T. I. Lin, V. D. Sled, T. Ohnishi, A. Brennicke, L. Grohmann, Analysis of the iron-sulfur clusters within the complex I (NADH:ubiquinone oxidoreductase) isolated

from potato tuber mitochondria. *European journal of biochemistry / FEBS* **230**, 1032-1036 (1995); published online EpubJun 15

22. K. Kita, H. Oya, R. B. Gennis, B. A. Ackrell, M. Kasahara, Human complex II (succinate-ubiquinone oxidoreductase): cDNA cloning of iron sulfur (Ip) subunit of liver mitochondria. *Biochemical and biophysical research communications* **166**, 101-108 (1990); published online EpubJan 15
23. R. L. Bell, R. A. Capaldi, The polypeptide composition of ubiquinone-cytochrome c reductase (complex III) from beef heart mitochondria. *Biochemistry* **15**, 996-1001 (1976); published online EpubMar 9
24. P. Gellerfors, M. Lunden, B. D. Nelson, Evidence for a function of core protein in complex III from beef-heart mitochondria. *European journal of biochemistry / FEBS* **67**, 463-468 (1976); published online EpubAug 16
25. K. Kita, S. Takamiya, R. Furushima, Y. C. Ma, H. Suzuki, T. Ozawa, H. Oya, Electron-transfer complexes of Ascaris suum muscle mitochondria. III. Composition and fumarate reductase activity of complex II. *Biochimica et biophysica acta* **935**, 130-140 (1988); published online EpubSep 14
26. N. Raimundo, B. E. Baysal, G. S. Shadel, Revisiting the TCA cycle: signaling to tumor formation. *Trends in molecular medicine* **17**, 641-649 (2011); published online EpubNov (10.1016/j.molmed.2011.06.001).
27. K. Inaba, A. Wakabayashi, T. Oda, Localization of TCA cycle dehydrogenases in the mitochondria. *Acta medicinae Okayama* **21**, 167-176 (1967); published online EpubAug
28. T. J. Piva, E. McEvoy-Bowe, The truncated TCA cycle in HeLa cell mitochondria. *Advances in experimental medicine and biology* **316**, 385-391 (1992).
29. H. Eubel, L. Jansch, H. P. Braun, New insights into the respiratory chain of plant mitochondria. Supercomplexes and a unique composition of complex II. *Plant physiology* **133**, 274-286 (2003); published online EpubSep
30. F. Daldal, E. Davidson, S. Cheng, Isolation of the structural genes for the Rieske Fe-S protein, cytochrome b and cytochrome c1 all components of the ubiquinol: cytochrome c2 oxidoreductase complex of Rhodopseudomonas capsulata. *Journal of molecular biology* **195**, 1-12 (1987); published online EpubMay 5
31. B. Schilling, J. Murray, C. B. Yoo, R. H. Row, M. P. Cusack, R. A. Capaldi, B. W. Gibson, Proteomic analysis of succinate dehydrogenase and ubiquinol-cytochrome c reductase (Complex II and III) isolated by immunoprecipitation from bovine and mouse heart mitochondria. *Biochimica et biophysica acta* **1762**, 213-222 (2006); published online EpubFeb (10.1016/j.bbadis.2005.07.003).
32. J. Haorah, T. J. Rump, H. Xiong, Reduction of brain mitochondrial beta-oxidation impairs complex I and V in chronic alcohol intake: the underlying mechanism for neurodegeneration. *PloS one* **8**, e70833 (2013)10.1371/journal.pone.0070833).

33. M. J. Luo, X. Y. He, H. Sprecher, H. Schulz, Purification and characterization of the trifunctional beta-oxidation complex from pig heart mitochondria. *Archives of biochemistry and biophysics* **304**, 266-271 (1993); published online EpubJul (10.1006/abbi.1993.1348).
34. K. L. Soole, I. B. Dry, J. T. Wiskich, Partial Purification and Characterization of Complex I, NADH:Ubiquinone Reductase, from the Inner Membrane of Beetroot Mitochondria. *Plant physiology* **98**, 588-594 (1992); published online EpubFeb
35. H. Hirawake, M. Taniwaki, A. Tamura, S. Kojima, K. Kita, Cytochrome b in human complex II (succinate-ubiquinone oxidoreductase): cDNA cloning of the components in liver mitochondria and chromosome assignment of the genes for the large (SDHC) and small (SDHD) subunits to 1q21 and 11q23. *Cytogenetics and cell genetics* **79**, 132-138 (1997).
36. P. Figueroa, G. Leon, A. Elorza, L. Holuigue, A. Araya, X. Jordana, The four subunits of mitochondrial respiratory complex II are encoded by multiple nuclear genes and targeted to mitochondria in Arabidopsis thaliana. *Plant molecular biology* **50**, 725-734 (2002); published online EpubNov
37. K. Kita, H. Hirawake, H. Miyadera, H. Amino, S. Takeo, Role of complex II in anaerobic respiration of the parasite mitochondria from Ascaris suum and Plasmodium falciparum. *Biochimica et biophysica acta* **1553**, 123-139 (2002); published online EpubJan 17
38. I. E. Scheffler, Molecular genetics of succinate:quinone oxidoreductase in eukaryotes. *Progress in nucleic acid research and molecular biology* **60**, 267-315 (1998).
39. J. Cheleski, H. J. Wiggers, A. P. Citadini, A. J. da Costa Filho, M. C. Nonato, C. A. Montanari, Kinetic mechanism and catalysis of Trypanosoma cruzi dihydroorotate dehydrogenase enzyme evaluated by isothermal titration calorimetry. *Analytical biochemistry* **399**, 13-22 (2010); published online EpubApr 1 (10.1016/j.ab.2009.11.018).
40. M. S. Baker, S. Bolis, D. A. Lowther, Oxidation of articular cartilage glyceraldehyde-3-phosphate dehydrogenase (G3PDH) occurs in vivo during carrageenin-induced arthritis. *Agents and actions* **32**, 299-304 (1991); published online EpubMar
41. M. Phelan, R. Boykins, I. Gray, Modification of glyceraldehyde-3-phosphate dehydrogenase, EC 1.2.1.12, isolated from rainbow trout during acclimation at 5 or 15 degrees C--II. Biochemical characterization of G3PDH muscle isolates. *Comparative biochemistry and physiology. B, Comparative biochemistry* **79**, 139-146 (1984).
42. W. Liu, J. M. Phang, Proline dehydrogenase (oxidase), a mitochondrial tumor suppressor, and autophagy under the hypoxia microenvironment. *Autophagy* **8**, 1407-1409 (2012); published online EpubSep (10.4161/auto.21152).

43. C. Servet, T. Ghelis, L. Richard, A. Zilberstein, A. Savoure, Proline dehydrogenase: a key enzyme in controlling cellular homeostasis. *Frontiers in bioscience* **17**, 607-620 (2012).
44. S. Wakai, M. Kikumoto, T. Kanao, K. Kamimura, Involvement of sulfide:quinone oxidoreductase in sulfur oxidation of an acidophilic iron-oxidizing bacterium, Acidithiobacillus ferrooxidans NASF-1. *Bioscience, biotechnology, and biochemistry* **68**, 2519-2528 (2004); published online EpubDec (10.1271/bbb.68.2519).
45. J. D. Beckmann, F. E. Frerman, Reaction of electron-transfer flavoprotein with electron-transfer flavoprotein-ubiquinone oxidoreductase. *Biochemistry* **24**, 3922-3925 (1985); published online EpubJul 16
46. Y. Diao, W. Lu, H. Jin, J. Zhu, L. Han, M. Xu, R. Gao, X. Shen, Z. Zhao, X. Liu, Y. Xu, J. Huang, H. Li, Discovery of diverse human dihydroorotate dehydrogenase inhibitors as immunosuppressive agents by structure-based virtual screening. *Journal of medicinal chemistry* **55**, 8341-8349 (2012); published online EpubOct 11 (10.1021/jm300630p).
47. T. A. Ismail, M. M. Soliman, M. A. Nassan, Molecular and immunohistochemical effects of metformin in a rat model of type 2 diabetes mellitus. *Experimental and therapeutic medicine* **9**, 1921-1930 (2015); published online EpubMay (10.3892/etm.2015.2354).
48. W. Liu, K. Glunde, Z. M. Bhujwalla, V. Raman, A. Sharma, J. M. Phang, Proline oxidase promotes tumor cell survival in hypoxic tumor microenvironments. *Cancer research* **72**, 3677-3686 (2012); published online EpubJul 15 (10.1158/0008-5472.CAN-12-0080).
49. W. Liu, C. N. Hancock, J. W. Fischer, M. Harman, J. M. Phang, Proline biosynthesis augments tumor cell growth and aerobic glycolysis: involvement of pyridine nucleotides. *Scientific reports* **5**, 17206 (2015)10.1038/srep17206).
50. W. Liu, O. Zabirnyk, H. Wang, Y. H. Shiao, M. L. Nickerson, S. Khalil, L. M. Anderson, A. O. Perantoni, J. M. Phang, miR-23b targets proline oxidase, a novel tumor suppressor protein in renal cancer. *Oncogene* **29**, 4914-4924 (2010); published online EpubSep 2 (10.1038/onc.2010.237).
51. M. Simkovic, G. D. Degala, S. S. Eaton, F. E. Frerman, Expression of human electron transfer flavoprotein-ubiquinone oxidoreductase from a baculovirus vector: kinetic and spectral characterization of the human protein. *The Biochemical journal* **364**, 659-667 (2002); published online EpubJun 15 (10.1042/BJ20020042).
52. N. Gregersen, B. S. Andresen, C. B. Pedersen, R. K. Olsen, T. J. Corydon, P. Bross, Mitochondrial fatty acid oxidation defects--remaining challenges. *Journal of inherited metabolic disease* **31**, 643-657 (2008); published online EpubOct (10.1007/s10545-008-0990-y).
53. R. K. Olsen, B. S. Andresen, E. Christensen, P. Bross, F. Skovby, N. Gregersen, Clear

relationship between ETF/ETFDH genotype and phenotype in patients with multiple acyl-CoA dehydrogenation deficiency. *Human mutation* **22**, 12-23 (2003); published online EpubJul (10.1002/humu.10226).

54. R. B. Bell, A. K. Brownell, C. R. Roe, A. G. Engel, S. I. Goodman, F. E. Frerman, D. W. Seccombe, F. F. Snyder, Electron transfer flavoprotein: ubiquinone oxidoreductase (ETF:QO) deficiency in an adult. *Neurology* **40**, 1779-1782 (1990); published online EpubNov
55. J. D. Beckmann, F. E. Frerman, Electron-transfer flavoprotein-ubiquinone oxidoreductase from pig liver: purification and molecular, redox, and catalytic properties. *Biochemistry* **24**, 3913-3921 (1985); published online EpubJul 16
56. S. I. Goodman, R. J. Binard, M. R. Woontner, F. E. Frerman, Glutaric acidemia type II: gene structure and mutations of the electron transfer flavoprotein:ubiquinone oxidoreductase (ETF:QO) gene. *Molecular genetics and metabolism* **77**, 86-90 (2002); published online EpubSep-Oct
57. H. Yan, D. W. Parsons, G. Jin, R. McLendon, B. A. Rasheed, W. Yuan, I. Kos, I. Batinic-Haberle, S. Jones, G. J. Riggins, H. Friedman, A. Friedman, D. Reardon, J. Herndon, K. W. Kinzler, V. E. Velculescu, B. Vogelstein, D. D. Bigner, IDH1 and IDH2 mutations in gliomas. *The New England journal of medicine* **360**, 765-773 (2009); published online EpubFeb 19 (10.1056/NEJMoa0808710).
58. L. Dang, D. W. White, S. Gross, B. D. Bennett, M. A. Bittinger, E. M. Driggers, V. R. Fantin, H. G. Jang, S. Jin, M. C. Keenan, K. M. Marks, R. M. Prins, P. S. Ward, K. E. Yen, L. M. Liau, J. D. Rabinowitz, L. C. Cantley, C. B. Thompson, M. G. Vander Heiden, S. M. Su, Cancer-associated IDH1 mutations produce 2-hydroxyglutarate. *Nature* **462**, 739-744 (2009); published online EpubDec 10 (10.1038/nature08617).
59. B. E. Baysal, R. E. Ferrell, J. E. Willett-Brozick, E. C. Lawrence, D. Myssiorek, A. Bosch, A. van der Mey, P. E. Taschner, W. S. Rubinstein, E. N. Myers, C. W. Richard, 3rd, C. J. Cornelisse, P. Devilee, B. Devlin, Mutations in SDHD, a mitochondrial complex II gene, in hereditary paraganglioma. *Science* **287**, 848-851 (2000); published online EpubFeb 4
60. F. E. Bleeker, N. A. Atai, S. Lamba, A. Jonker, D. Rijkeboer, K. S. Bosch, W. Tigchelaar, D. Troost, W. P. Vandertop, A. Bardelli, C. J. Van Noorden, The prognostic IDH1(R132) mutation is associated with reduced NADP+-dependent IDH activity in glioblastoma. *Acta neuropathologica* **119**, 487-494 (2010); published online EpubApr (10.1007/s00401-010-0645-6).
61. P. J. Pollard, J. J. Briere, N. A. Alam, J. Barwell, E. Barclay, N. C. Wortham, T. Hunt, M. Mitchell, S. Olpin, S. J. Moat, I. P. Hargreaves, S. J. Heales, Y. L. Chung, J. R. Griffiths, A. Dalgleish, J. A. McGrath, M. J. Gleeson, S. V. Hodgson, R. Poulsom, P. Rustin, I. P. Tomlinson, Accumulation of Krebs cycle intermediates and over-expression of HIF1alpha in tumours which result from germline FH and SDH

mutations. *Human molecular genetics* **14**, 2231-2239 (2005); published online EpubAug 1 (10.1093/hmg/ddi227).

62. M. A. Selak, S. M. Armour, E. D. MacKenzie, H. Boulahbel, D. G. Watson, K. D. Mansfield, Y. Pan, M. C. Simon, C. B. Thompson, E. Gottlieb, Succinate links TCA cycle dysfunction to oncogenesis by inhibiting HIF-alpha prolyl hydroxylase. *Cancer cell* **7**, 77-85 (2005); published online EpubJan (10.1016/j.ccr.2004.11.022).
63. S. Sudarshan, W. M. Linehan, L. Neckers, HIF and fumarate hydratase in renal cancer. *British journal of cancer* **96**, 403-407 (2007); published online EpubFeb 12 (10.1038/sj.bjc.6603547).
64. G. Zhao, Y. Liu, J. Fang, Y. Chen, H. Li, K. Gao, Dimethyl fumarate inhibits the expression and function of hypoxia-inducible factor-1alpha (HIF-1alpha). *Biochemical and biophysical research communications* **448**, 303-307 (2014); published online EpubJun 6 (10.1016/j.bbrc.2014.02.062).
65. Y. Hakak, K. Lehmann-Bruinsma, S. Phillips, T. Le, C. Liaw, D. T. Connolly, D. P. Behan, The role of the GPR91 ligand succinate in hematopoiesis. *Journal of leukocyte biology* **85**, 837-843 (2009); published online EpubMay (10.1189/jlb.1008618).
66. A. P. Gimenez-Roqueplo, N. Burnichon, L. Amar, J. Favier, X. Jeunemaitre, P. F. Plouin, Recent advances in the genetics of phaeochromocytoma and functional paraganglioma. *Clinical and experimental pharmacology & physiology* **35**, 376-379 (2008); published online EpubApr (10.1111/j.1440-1681.2008.04881.x).
67. E. A. Berry, L. S. Huang, V. J. DeRose, Ubiquinol-cytochrome c oxidoreductase of higher plants. Isolation and characterization of the bc1 complex from potato tuber mitochondria. *The Journal of biological chemistry* **266**, 9064-9077 (1991); published online EpubMay 15
68. D. K. Inaoka, T. Shiba, D. Sato, E. O. Balogun, T. Sasaki, M. Nagahama, M. Oda, S. Matsuoka, J. Ohmori, T. Honma, M. Inoue, K. Kita, S. Harada, Structural Insights into the Molecular Design of Flutolanil Derivatives Targeted for Fumarate Respiration of Parasite Mitochondria. *International journal of molecular sciences* **16**, 15287-15308 (2015)10.3390/ijms160715287).
69. E. Tomitsuka, K. Kita, H. Esumi, An anticancer agent, pyrvinium pamoate inhibits the NADH-fumarate reductase system--a unique mitochondrial energy metabolism in tumour microenvironments. *Journal of biochemistry* **152**, 171-183 (2012); published online EpubAug (10.1093/jb/mvs041).
70. E. Maklashina, G. Cecchini, S. A. Dikanov, Defining a direction: electron transfer and catalysis in Escherichia coli complex II enzymes. *Biochimica et biophysica acta* **1827**, 668-678 (2013); published online EpubMay (10.1016/j.bbabio.2013.01.010).
71. G. M. Cook, K. Hards, C. Vilcheze, T. Hartman, M. Berney, Energetics of Respiration and Oxidative Phosphorylation in Mycobacteria. *Microbiology spectrum* **2**, (2014);

published online EpubJun (10.1128/microbiolspec.MGM2-0015-2013).

72. T. Okano, Y. Shimomura, M. Yamane, Y. Suhara, M. Kamao, M. Sugiura, K. Nakagawa, Conversion of phylloquinone (Vitamin K1) into menaquinone-4 (Vitamin K2) in mice: two possible routes for menaquinone-4 accumulation in cerebra of mice. *The Journal of biological chemistry* **283**, 11270-11279 (2008); published online EpubApr 25 (10.1074/jbc.M702971200).
73. J. J. Van Hellemond, F. R. Opperdoes, A. G. Tielens, Trypanosomatidae produce acetate via a mitochondrial acetate:succinate CoA transferase. *Proceedings of the National Academy of Sciences of the United States of America* **95**, 3036-3041 (1998); published online EpubMar 17
74. Y. Millerioux, P. Morand, M. Biran, M. Mazet, P. Moreau, M. Wargnies, C. Ebikeme, K. Deramchia, L. Gales, J. C. Portais, M. Boshart, J. M. Franconi, F. Bringaud, ATP synthesis-coupled and -uncoupled acetate production from acetyl-CoA by mitochondrial acetate:succinate CoA-transferase and acetyl-CoA thioesterase in Trypanosoma. *The Journal of biological chemistry* **287**, 17186-17197 (2012); published online EpubMay 18 (10.1074/jbc.M112.355404).
75. K. W. van Grinsven, S. Rosnowsky, S. W. van Weelden, S. Putz, M. van der Giezen, W. Martin, J. J. van Hellemond, A. G. Tielens, K. Henze, Acetate:succinate CoA-transferase in the hydrogenosomes of Trichomonas vaginalis: identification and characterization. *The Journal of biological chemistry* **283**, 1411-1418 (2008); published online EpubJan 18 (10.1074/jbc.M702528200).
76. K. W. van Grinsven, J. J. van Hellemond, A. G. Tielens, Acetate:succinate CoA-transferase in the anaerobic mitochondria of Fasciola hepatica. *Molecular and biochemical parasitology* **164**, 74-79 (2009); published online EpubMar (10.1016/j.molbiopara.2008.11.008).
77. A. G. Tielens, K. W. van Grinsven, K. Henze, J. J. van Hellemond, W. Martin, Acetate formation in the energy metabolism of parasitic helminths and protists. *International journal for parasitology* **40**, 387-397 (2010); published online EpubMar 15 (10.1016/j.ijpara.2009.12.006).
78. J. Huang, M. Malhi, J. Deneke, M. E. Fraser, Structure of GTP-specific succinyl-CoA synthetase in complex with CoA. *Acta crystallographica. Section F, Structural biology communications* **71**, 1067-1071 (2015); published online EpubAug (10.1107/S2053230X15011188).
79. M. A. Joyce, M. E. Fraser, M. N. James, W. A. Bridger, W. T. Wolodko, ADP-binding site of Escherichia coli succinyl-CoA synthetase revealed by x-ray crystallography. *Biochemistry* **39**, 17-25 (2000); published online EpubJan 11
80. R. B. Mythri, B. Jagatha, N. Pradhan, J. Andersen, M. M. Bharath, Mitochondrial complex I inhibition in Parkinson's disease: how can curcumin protect mitochondria? *Antioxidants & redox signaling* **9**, 399-408 (2007); published online EpubMar

(10.1089/ars.2007.9.ft-25).

81. S. Y. Jin, H. S. Lee, E. K. Kim, J. M. Ha, Y. W. Kim, S. Bae, Reactive oxygen species and PI3K/Akt signaling in cancer. *Free radical biology & medicine* **75 Suppl 1**, S34-35 (2014); published online EpubOct (10.1016/j.freeradbiomed.2014.10.773).
82. B. Joshi, L. Li, B. G. Taffe, Z. Zhu, S. Wahl, H. Tian, E. Ben-Josef, J. D. Taylor, A. T. Porter, D. G. Tang, Apoptosis induction by a novel anti-prostate cancer compound, BMD188 (a fatty acid-containing hydroxamic acid), requires the mitochondrial respiratory chain. *Cancer research* **59**, 4343-4355 (1999); published online EpubSep 1
83. J. H. Lee, Y. S. Won, K. H. Park, M. K. Lee, H. Tachibana, K. Yamada, K. I. Seo, Celastrol inhibits growth and induces apoptotic cell death in melanoma cells via the activation ROS-dependent mitochondrial pathway and the suppression of PI3K/AKT signaling. *Apoptosis : an international journal on programmed cell death* **17**, 1275-1286 (2012); published online EpubDec (10.1007/s10495-012-0767-5).
84. M. D. Seidman, W. S. Quirk, N. A. Shirwany, Reactive oxygen metabolites, antioxidants and head and neck cancer. *Head & neck* **21**, 467-479 (1999); published online EpubAug
85. X. Yuan, Y. Zhou, W. Wang, J. Li, G. Xie, Y. Zhao, D. Xu, L. Shen, Activation of TLR4 signaling promotes gastric cancer progression by inducing mitochondrial ROS production. *Cell death & disease* **4**, e794 (2013)10.1038/cddis.2013.334).
86. I. Syed, C. N. Kyathanahalli, B. Jayaram, S. Govind, C. J. Rhodes, R. A. Kowluru, A. Kowluru, Increased phagocyte-like NADPH oxidase and ROS generation in type 2 diabetic ZDF rat and human islets: role of Rac1-JNK1/2 signaling pathway in mitochondrial dysregulation in the diabetic islet. *Diabetes* **60**, 2843-2852 (2011); published online EpubNov (10.2337/db11-0809).
87. C. Yang, C. C. Aye, X. Li, A. Diaz Ramos, A. Zorzano, S. Mora, Mitochondrial dysfunction in insulin resistance: differential contributions of chronic insulin and saturated fatty acid exposure in muscle cells. *Bioscience reports* **32**, 465-478 (2012); published online EpubOct (10.1042/BSR20120034).
88. E. P. Rhee, NADPH Oxidase 4 at the Nexus of Diabetes, Reactive Oxygen Species, and Renal Metabolism. *Journal of the American Society of Nephrology : JASN*, (2015); published online EpubJul 22 (10.1681/ASN.2015060698).
89. Y. Shi, P. M. Vanhoutte, Reactive oxygen-derived free radicals are key to the endothelial dysfunction of diabetes. *Journal of diabetes* **1**, 151-162 (2009); published online EpubSep (10.1111/j.1753-0407.2009.00030.x).
90. V. J. Adlam, J. C. Harrison, C. M. Porteous, A. M. James, R. A. Smith, M. P. Murphy, I. A. Sammut, Targeting an antioxidant to mitochondria decreases cardiac ischemia-reperfusion injury. *FASEB journal : official publication of the Federation of American Societies for Experimental Biology* **19**, 1088-1095 (2005); published online EpubJul (10.1096/fj.05-3718com).

91. E. J. Lesnefsky, C. L. Hoppel, Ischemia-reperfusion injury in the aged heart: role of mitochondria. *Archives of biochemistry and biophysics* **420**, 287-297 (2003); published online EpubDec 15
92. W. Q. Tian, Y. G. Peng, S. Y. Cui, F. Z. Yao, B. G. Li, Effects of electroacupuncture of different intensities on energy metabolism of mitochondria of brain cells in rats with cerebral ischemia-reperfusion injury. *Chinese journal of integrative medicine* **21**, 618-623 (2015); published online EpubAug (10.1007/s11655-013-1512-9).
93. A. Kornberg, U. Witt, J. Kornberg, H. Friess, K. Thrum, Treating ischaemia-reperfusion injury with prostaglandin E1 reduces the risk of early hepatocellular carcinoma recurrence following liver transplantation. *Alimentary pharmacology & therapeutics* **42**, 1101-1110 (2015); published online EpubNov (10.1111/apt.13380).
94. S. Jegatheeswaran, S. Jamdar, T. Satyadas, A. J. Sheen, R. Adam, A. K. Siriwardena, Use of Pharmacologic Agents for Modulation of Ischaemia-Reperfusion Injury after Hepatectomy: A Questionnaire Study of the LiverMetSurvey International Registry of Hepatic Surgery Units. *HPB surgery : a world journal of hepatic, pancreatic and biliary surgery* **2014**, 437159 (2014)10.1155/2014/437159).
95. A. Fukuda, S. Okubo, Y. Tanabe, Y. Hoshiba, H. Shiobara, K. Harafuji, Y. Kobori, M. Fujinawa, T. Okubo, A. Yamashina, Cardioprotective effect of edaravone against ischaemia-reperfusion injury in the rabbit heart before, during and after reperfusion treatment. *The Journal of international medical research* **34**, 475-484 (2006); published online EpubSep-Oct
96. Y. R. Liu, P. W. Li, J. J. Suo, Y. Sun, B. A. Zhang, H. Lu, H. C. Zhu, G. B. Zhang, Catalpol provides protective effects against cerebral ischaemia/reperfusion injury in gerbils. *The Journal of pharmacy and pharmacology* **66**, 1265-1270 (2014); published online EpubSep (10.1111/jphp.12261).
97. P. W. Ho, W. F. Pang, C. C. Szeto, Remote ischemic pre-conditioning for the prevention of acute kidney injury. *Nephrology*, (2015); published online EpubSep 15 (10.1111/nep.12614).
98. J. S. Kim, J. H. Wang, J. J. Lemasters, Mitochondrial permeability transition in rat hepatocytes after anoxia/reoxygenation: role of Ca2+-dependent mitochondrial formation of reactive oxygen species. *American journal of physiology. Gastrointestinal and liver physiology* **302**, G723-731 (2012); published online EpubApr (10.1152/ajpgi.00082.2011).
99. N. R. Jena, P. C. Mishra, Mechanisms of formation of 8-oxoguanine due to reactions of one and two OH* radicals and the H2O2 molecule with guanine: A quantum computational study. *The journal of physical chemistry. B* **109**, 14205-14218 (2005); published online EpubJul 28 (10.1021/jp050646j).
100. B. A. Miller, N. E. Hoffman, S. Merali, X. Q. Zhang, J. Wang, S. Rajan, S.

Shanmughapriya, E. Gao, C. A. Barrero, K. Mallilankaraman, J. Song, T. Gu, I. Hirschler-Laszkiewicz, W. J. Koch, A. M. Feldman, M. Madesh, J. Y. Cheung, TRPM2 channels protect against cardiac ischemia-reperfusion injury: role of mitochondria. *The Journal of biological chemistry* **289**, 7615-7629 (2014); published online EpubMar 14 (10.1074/jbc.M113.533851).

101. O. Ertracht, A. Malka, S. Atar, O. Binah, The mitochondria as a target for cardioprotection in acute myocardial ischemia. *Pharmacology & therapeutics* **142**, 33-40 (2014); published online EpubApr (10.1016/j.pharmthera.2013.11.003).
102. C. Montessuit, I. Papageorgiou, I. Tardy-Cantalupi, N. Rosenblatt-Velin, R. Lerch, Postischemic recovery of heart metabolism and function: role of mitochondrial fatty acid transfer. *Journal of applied physiology* **89**, 111-119 (2000); published online EpubJul
103. M. A. Perez-Pinzon, G. P. Xu, J. Born, J. Lorenzo, R. Busto, M. Rosenthal, T. J. Sick, Cytochrome C is released from mitochondria into the cytosol after cerebral anoxia or ischemia. *Journal of cerebral blood flow and metabolism : official journal of the International Society of Cerebral Blood Flow and Metabolism* **19**, 39-43 (1999); published online EpubJan (10.1097/00004647-199901000-00004).
104. P. Zhao, F. Li, W. Gao, J. Wang, L. Fu, Y. Chen, M. Huang, Angiotensin1-7 protects cardiomyocytes from hypoxia/reoxygenation-induced oxidative stress by preventing ROS-associated mitochondrial dysfunction and activating the Akt signaling pathway. *Acta histochemica* **117**, 803-810 (2015); published online EpubOct (10.1016/j.acthis.2015.07.004).
105. M. F. Anderson, N. R. Sims, The effects of focal ischemia and reperfusion on the glutathione content of mitochondria from rat brain subregions. *Journal of neurochemistry* **81**, 541-549 (2002); published online EpubMay
106. M. Christophe, S. Nicolas, Mitochondria: a target for neuroprotective interventions in cerebral ischemia-reperfusion. *Current pharmaceutical design* **12**, 739-757 (2006).
107. C. Stella, I. Burgos, S. Chapela, O. Gamondi, Ischemia--reperfusion: a look from yeast mitochondria. *Current medicinal chemistry* **18**, 3476-3484 (2011).
108. E. T. Chouchani, V. R. Pell, E. Gaude, D. Aksentijevic, S. Y. Sundier, E. L. Robb, A. Logan, S. M. Nadtochiy, E. N. Ord, A. C. Smith, F. Eyassu, R. Shirley, C. H. Hu, A. J. Dare, A. M. James, S. Rogatti, R. C. Hartley, S. Eaton, A. S. Costa, P. S. Brookes, S. M. Davidson, M. R. Duchen, K. Saeb-Parsy, M. J. Shattock, A. J. Robinson, L. M. Work, C. Frezza, T. Krieg, M. P. Murphy, Ischaemic accumulation of succinate controls reperfusion injury through mitochondrial ROS. *Nature* **515**, 431-435 (2014); published online EpubNov 20 (10.1038/nature13909).
109. R. F. Villa, A. Gorini, F. Ferrari, S. Hoyer, Energy metabolism of cerebral mitochondria during aging, ischemia and post-ischemic recovery assessed by functional proteomics of enzymes. *Neurochemistry international* **63**, 765-781 (2013);

published online EpubDec (10.1016/j.neuint.2013.10.004).

110. C. L. Chen, J. Chen, S. Rawale, S. Varadharaj, P. P. Kaumaya, J. L. Zweier, Y. R. Chen, Protein tyrosine nitration of the flavin subunit is associated with oxidative modification of mitochondrial complex II in the post-ischemic myocardium. *The Journal of biological chemistry* **283**, 27991-28003 (2008); published online EpubOct 10 (10.1074/jbc.M802691200).
111. J. R. Koenitzer, G. Bonacci, S. R. Woodcock, C. S. Chen, N. Cantu-Medellin, E. E. Kelley, F. J. Schopfer, Fatty acid nitroalkenes induce resistance to ischemic cardiac injury by modulating mitochondrial respiration at complex II. *Redox biology* **8**, 1-10 (2015); published online EpubNov 17 (10.1016/j.redox.2015.11.002).
112. L. Zhang, C. L. Chen, P. T. Kang, V. Garg, K. Hu, K. B. Green-Church, Y. R. Chen, Peroxynitrite-mediated oxidative modifications of complex II: relevance in myocardial infarction. *Biochemistry* **49**, 2529-2539 (2010); published online EpubMar 23 (10.1021/bi9018237).
113. E. Tomitsuka, Y. Goto, M. Taniwaki, K. Kita, Direct evidence for expression of type II flavoprotein subunit in human complex II (succinate-ubiquinone reductase). *Biochemical and biophysical research communications* **311**, 774-779 (2003); published online EpubNov 21
114. J. Hu, Q. Wu, T. Li, Y. Chen, S. Wang, Inhibition of high glucose-induced VEGF release in retinal ganglion cells by RNA interference targeting G protein-coupled receptor 91. *Experimental eye research* **109**, 31-39 (2013); published online EpubApr (10.1016/j.exer.2013.01.011).
115. K. Brockmann, A. Bjornstad, P. Dechent, C. G. Korenke, J. Smeitink, J. M. Trijbels, S. Athanassopoulos, R. Villagran, O. H. Skjeldal, E. Wilichowski, J. Frahm, F. Hanefeld, Succinate in dystrophic white matter: a proton magnetic resonance spectroscopy finding characteristic for complex II deficiency. *Annals of neurology* **52**, 38-46 (2002); published online EpubJul (10.1002/ana.10232).
116. I. Toma, J. J. Kang, A. Sipos, S. Vargas, E. Bansal, F. Hanner, E. Meer, J. Peti-Peterdi, Succinate receptor GPR91 provides a direct link between high glucose levels and renin release in murine and rabbit kidney. *The Journal of clinical investigation* **118**, 2526-2534 (2008); published online EpubJul (10.1172/JCI33293).
117. H. Busch, V. R. Potter, Succinate accumulation in vivo following injection of malonate. *The Journal of biological chemistry* **198**, 71-77 (1952); published online EpubSep
118. D. Valverde, M. R. Quintero, A. P. Candiota, L. Badiella, M. E. Cabanas, C. Arus, Analysis of the changes in the 1H NMR spectral pattern of perchloric acid extracts of C6 cells with growth. *NMR in biomedicine* **19**, 223-230 (2006); published online EpubApr (10.1002/nbm.1024).
119. W. He, F. J. Miao, D. C. Lin, R. T. Schwandner, Z. Wang, J. Gao, J. L. Chen, H. Tian, L. Ling, Citric acid cycle intermediates as ligands for orphan G-protein-coupled

receptors. *Nature* **429**, 188-193 (2004); published online EpubMay 13 (10.1038/nature02488).

120. C. N. Alves, J. R. Silva, A. E. Roitberg, Insights into the mechanism of oxidation of dihydroorotate to orotate catalysed by human class 2 dihydroorotate dehydrogenase: a QM/MM free energy study. *Physical chemistry chemical physics : PCCP* **17**, 17790-17796 (2015); published online EpubJul 21 (10.1039/c5cp02016f).
121. O. Bjornberg, D. B. Jordan, B. A. Palfey, K. F. Jensen, Dihydrooxonate is a substrate of dihydroorotate dehydrogenase (DHOD) providing evidence for involvement of cysteine and serine residues in base catalysis. *Archives of biochemistry and biophysics* **391**, 286-294 (2001); published online EpubJul 15 (10.1006/abbi.2001.2409).
122. I. Ben-Sahra, J. J. Howell, J. M. Asara, B. D. Manning, Stimulation of de novo pyrimidine synthesis by growth signaling through mTOR and S6K1. *Science* **339**, 1323-1328 (2013); published online EpubMar 15 (10.1126/science.1228792).
123. M. Huang, L. M. Graves, De novo synthesis of pyrimidine nucleotides; emerging interfaces with signal transduction pathways. *Cellular and molecular life sciences : CMLS* **60**, 321-336 (2003); published online EpubFeb
124. Y. Wang, C. Cherian, S. Orr, S. Mitchell-Ryan, Z. Hou, S. Raghavan, L. H. Matherly, A. Gangjee, Tumor-targeting with novel non-benzoyl 6-substituted straight chain pyrrolo[2,3-d]pyrimidine antifolates via cellular uptake by folate receptor alpha and inhibition of de novo purine nucleotide biosynthesis. *Journal of medicinal chemistry* **56**, 8684-8695 (2013); published online EpubNov 14 (10.1021/jm401139z).
125. E. Bonke, K. Zwicker, S. Drose, Manganese ions induce H2O2 generation at the ubiquinone binding site of mitochondrial complex II. *Archives of biochemistry and biophysics* **580**, 75-83 (2015); published online EpubAug 15 (10.1016/j.abb.2015.06.011).
126. A. Anderson, A. Bowman, S. J. Boulton, P. Manning, M. A. Birch-Machin, A role for human mitochondrial complex II in the production of reactive oxygen species in human skin. *Redox biology* **2C**, 1016-1022 (2014); published online EpubAug 28 (10.1016/j.redox.2014.08.005).
127. M. Forkink, F. Basit, J. Teixeira, H. G. Swarts, W. J. Koopman, P. H. Willems, Complex I and complex III inhibition specifically increase cytosolic hydrogen peroxide levels without inducing oxidative stress in HEK293 cells. *Redox biology* **6**, 607-616 (2015); published online EpubDec (10.1016/j.redox.2015.09.003).
128. N. Nouraee, S. Khazaei, M. Vasei, S. F. Razavipour, M. Sadeghizadeh, S. J. Mowla, MicroRNAs contribution in tumor microenvironment of esophageal cancer. *Cancer biomarkers : section A of Disease markers*, (2016); published online EpubFeb 2 (10.3233/CBM-160575).
129. B. R. Achyut, A. Shankar, A. S. Iskander, R. Ara, R. A. Knight, A. G. Scicli, A. S. Arbab,

Chimeric Mouse Model to Track the Migration of Bone Marrow Derived Cells in Glioblastoma Following Anti-angiogenic Treatments. *Cancer biology & therapy*, 0 (2016); published online EpubJan 21 (10.1080/15384047.2016.1139243).

130. R. Bulla, C. Tripodo, D. Rami, G. S. Ling, C. Agostinis, C. Guarnotta, S. Zorzet, P. Durigutto, M. Botto, F. Tedesco, C1q acts in the tumour microenvironment as a cancer-promoting factor independently of complement activation. *Nature communications* **7**, 10346 (2016)10.1038/ncomms10346).
131. J. Song, L. Feng, R. Zhong, Z. Xia, L. Zhang, L. Cui, H. Yan, X. Jia, Z. Zhang, Icariside II inhibits the EMT of NSCLC cells in inflammatory microenvironment via down-regulation of Akt/NF-kappaB signaling pathway. *Molecular carcinogenesis*, (2016); published online EpubFeb 9 (10.1002/mc.22471).
132. S. K. Jeong, J. S. Kim, C. G. Lee, Y. S. Park, S. D. Kim, S. O. Yoon, D. H. Han, K. Y. Lee, M. H. Jeong, W. S. Jo, Tumor associated macrophages provide the survival resistance of tumor cells to hypoxic microenvironmental condition through IL-6 receptor-mediated signals. *Immunobiology*, (2015); published online EpubNov 27 (10.1016/j.imbio.2015.11.010).
133. M. Akimoto, J. I. Hayashi, S. Nakae, H. Saito, K. Takenaga, Interleukin-33 enhances programmed oncosis of ST2L-positive low-metastatic cells in the tumour microenvironment of lung cancer. *Cell death & disease* **7**, e2057 (2016)10.1038/cddis.2015.418).
134. M. Catarinella, A. Monestiroli, G. Escobar, A. Fiocchi, N. L. Tran, R. Aiolfi, P. Marra, A. Esposito, F. Cipriani, L. Aldrighetti, M. Iannacone, L. Naldini, L. G. Guidotti, G. Sitia, IFNalpha gene/cell therapy curbs colorectal cancer colonization of the liver by acting on the hepatic microenvironment. *EMBO molecular medicine* **8**, 155-170 (2016)10.15252/emmm.201505395).
135. J. S. Lee, J. H. Kang, H. J. Boo, S. J. Hwang, S. Hong, S. C. Lee, Y. J. Park, T. M. Chung, H. Youn, S. M. Lee, B. J. Kim, J. K. Chung, Y. Chung, W. N. William, Jr., Y. K. Shin, H. J. Lee, S. H. Oh, H. Y. Lee, STAT3-mediated IGF-2 secretion in the tumour microenvironment elicits innate resistance to anti-IGF-1R antibody. *Nature communications* **6**, 8499 (2015)10.1038/ncomms9499).
136. H. Y. Yang, R. M. Qu, X. S. Lin, T. X. Liu, Q. Q. Sun, C. Yang, X. H. Li, W. Lu, X. F. Hu, J. X. Dai, L. Yuan, IGF-1 from adipose-derived mesenchymal stem cells promotes radioresistance of breast cancer cells. *Asian Pacific journal of cancer prevention : APJCP* **15**, 10115-10119 (2014).
137. Y. You, Y. Shan, J. Chen, H. Yue, B. You, S. Shi, X. Li, X. Cao, Matrix metalloproteinase 13-containing exosomes promote nasopharyngeal carcinoma metastasis. *Cancer science* **106**, 1669-1677 (2015); published online EpubDec (10.1111/cas.12818).
138. M. Herrera-Perez, S. L. Voytik-Harbin, J. L. Rickus, Extracellular Matrix Properties

Regulate the Migratory Response of Glioblastoma Stem Cells in Three-Dimensional Culture. *Tissue engineering. Part A* **21**, 2572-2582 (2015); published online EpubOct (10.1089/ten.TEA.2014.0504).

139. B. Heissig, D. Dhahri, S. Eiamboonsert, Y. Salama, H. Shimazu, S. Munakata, K. Hattori, Role of mesenchymal stem cell-derived fibrinolytic factor in tissue regeneration and cancer progression. *Cellular and molecular life sciences : CMLS* **72**, 4759-4770 (2015); published online EpubDec (10.1007/s00018-015-2035-7).
140. S. K. Parks, Y. Cormerais, I. Marchiq, J. Pouyssegur, Hypoxia optimises tumour growth by controlling nutrient import and acidic metabolite export. *Molecular aspects of medicine* **47-48**, 3-14 (2016); published online EpubFeb-Mar (10.1016/j.mam.2015.12.001).
141. N. M. da Costa, A. D. Fialho, C. C. Proietti, M. S. Kataoka, R. G. Jaeger, S. M. de Alves-Junior, J. J. Pinheiro, Role of hypoxia-related proteins in invasion of ameloblastoma cells: crosstalk between NOTCH1, HIF-1alpha, ADAM-12, and HB-EGF. *Histopathology*, (2015); published online EpubDec 28 (10.1111/his.12922).
142. M. Li, M. Li, T. Yin, H. Shi, Y. Wen, B. Zhang, M. Chen, G. Xu, K. Ren, Y. Wei, Targeting of cancerassociated fibroblasts enhances the efficacy of cancer chemotherapy by regulating the tumor microenvironment. *Molecular medicine reports*, (2016); published online EpubFeb 4 (10.3892/mmr.2016.4868).
143. M. J. McCoy, C. Hemmings, T. J. Miller, S. J. Austin, M. K. Bulsara, N. Zeps, A. K. Nowak, R. A. Lake, C. F. Platell, Low stromal Foxp3(+) regulatory T-cell density is associated with complete response to neoadjuvant chemoradiotherapy in rectal cancer. *British journal of cancer* **113**, 1677-1686 (2015); published online EpubDec 22 (10.1038/bjc.2015.427).
144. J. A. Spencer, F. Ferraro, E. Roussakis, A. Klein, J. Wu, J. M. Runnels, W. Zaher, L. J. Mortensen, C. Alt, R. Turcotte, R. Yusuf, D. Cote, S. A. Vinogradov, D. T. Scadden, C. P. Lin, Direct measurement of local oxygen concentration in the bone marrow of live animals. *Nature* **508**, 269-273 (2014); published online EpubApr 10 (10.1038/nature13034).
145. I. Momose, S. Ohba, D. Tatsuda, M. Kawada, T. Masuda, G. Tsujiuchi, T. Yamori, H. Esumi, D. Ikeda, Mitochondrial inhibitors show preferential cytotoxicity to human pancreatic cancer PANC-1 cells under glucose-deprived conditions. *Biochemical and biophysical research communications* **392**, 460-466 (2010); published online EpubFeb 12 (10.1016/j.bbrc.2010.01.050).
146. F. Zoccarato, L. Cavallini, S. Bortolami, A. Alexandre, Succinate modulation of H2O2 release at NADH:ubiquinone oxidoreductase (Complex I) in brain mitochondria. *The Biochemical journal* **406**, 125-129 (2007); published online EpubAug 15 (10.1042/BJ20070215).
147. C. Stamm, I. Friehs, Y. H. Choi, D. Zurakowski, F. X. McGowan, P. J. del Nido,

Cytosolic calcium in the ischemic rabbit heart: assessment by pH- and temperature-adjusted rhod-2 spectrofluorometry. *Cardiovascular research* **59**, 695-704 (2003); published online EpubSep 1

148. K. Setsukinai, Y. Urano, K. Kakinuma, H. J. Majima, T. Nagano, Development of novel fluorescence probes that can reliably detect reactive oxygen species and distinguish specific species. *The Journal of biological chemistry* **278**, 3170-3175 (2003); published online EpubJan 31 (10.1074/jbc.M209264200).
149. K. E. Oberg, The Inhibition of the Respiration of Brain Mitochondria of Rotenone-Poisoned Fish. *Experimental cell research* **36**, 407-410 (1964); published online EpubNov
150. M. L. Genova, C. Bovina, M. Marchetti, F. Pallotti, C. Tietz, G. Biagini, A. Pugnaloni, C. Viticchi, A. Gorini, R. F. Villa, G. Lenaz, Decrease of rotenone inhibition is a sensitive parameter of complex I damage in brain non-synaptic mitochondria of aged rats. *FEBS letters* **410**, 467-469 (1997); published online EpubJun 30
151. T. P. Selby, K. A. Hughes, J. J. Rauh, W. S. Hanna, Synthetic atpenin analogs: Potent mitochondrial inhibitors of mammalian and fungal succinate-ubiquinone oxidoreductase. *Bioorganic & medicinal chemistry letters* **20**, 1665-1668 (2010); published online EpubMar 1 (10.1016/j.bmcl.2010.01.066).
152. A. P. Wojtovich, P. S. Brookes, The complex II inhibitor atpenin A5 protects against cardiac ischemia-reperfusion injury via activation of mitochondrial KATP channels. *Basic research in cardiology* **104**, 121-129 (2009); published online EpubMar (10.1007/s00395-009-0001-y).
153. E. Prahoveanu, M. Gruia, R. Lupu, N. Cajal, The effect of malonate on succinic dehydrogenase (SDH) activity during the multiplication of influenza and herpes viruses in the embryonate hen egg. *Revue roumaine de virologie* **25**, 247-253 (1974).
154. M. Saint-Macary, B. Foucher, Binding of malonate to the inner membrane of rat liver mitochondria. *Biochemical and biophysical research communications* **96**, 457-462 (1980); published online EpubSep 16
155. S. Iwata, J. W. Lee, K. Okada, J. K. Lee, M. Iwata, B. Rasmussen, T. A. Link, S. Ramaswamy, B. K. Jap, Complete structure of the 11-subunit bovine mitochondrial cytochrome bc1 complex. *Science* **281**, 64-71 (1998); published online EpubJul 3
156. H. M. Peshavariya, G. J. Dusting, S. Selemidis, Analysis of dihydroethidium fluorescence for the detection of intracellular and extracellular superoxide produced by NADPH oxidase. *Free radical research* **41**, 699-712 (2007); published online EpubJun (10.1080/10715760701297354).
157. T. Ueno, Y. Urano, K. Setsukinai, H. Takakusa, H. Kojima, K. Kikuchi, K. Ohkubo, S. Fukuzumi, T. Nagano, Rational principles for modulating fluorescence properties of fluorescein. *Journal of the American Chemical Society* **126**, 14079-14085 (2004); published online EpubNov 3 (10.1021/ja048241k).

158. C. O. Park, X. H. Xiao, D. G. Allen, Changes in intracellular Na+ and pH in rat heart during ischemia: role of Na+/H+ exchanger. *The American journal of physiology* **276**, H1581-1590 (1999); published online EpubMay
159. R. F. Villa, A. Gorini, S. Hoyer, Effect of ageing and ischemia on enzymatic activities linked to Krebs' cycle, electron transfer chain, glutamate and aminoacids metabolism of free and intrasynaptic mitochondria of cerebral cortex. *Neurochemical research* **34**, 2102-2116 (2009); published online EpubDec (10.1007/s11064-009-0004-y).
160. E. Cadenas, K. J. Davies, Mitochondrial free radical generation, oxidative stress, and aging. *Free radical biology & medicine* **29**, 222-230 (2000); published online EpubAug
161. Q. Chen, E. J. Vazquez, S. Moghaddas, C. L. Hoppel, E. J. Lesnefsky, Production of reactive oxygen species by mitochondria: central role of complex III. *The Journal of biological chemistry* **278**, 36027-36031 (2003); published online EpubSep 19 (10.1074/jbc.M304854200).
162. J. St-Pierre, J. A. Buckingham, S. J. Roebuck, M. D. Brand, Topology of superoxide production from different sites in the mitochondrial electron transport chain. *The Journal of biological chemistry* **277**, 44784-44790 (2002); published online EpubNov 22 (10.1074/jbc.M207217200).
163. P. Caro, J. Gomez, I. Sanchez, A. Naudi, V. Ayala, M. Lopez-Torres, R. Pamplona, G. Barja, Forty percent methionine restriction decreases mitochondrial oxygen radical production and leak at complex I during forward electron flow and lowers oxidative damage to proteins and mitochondrial DNA in rat kidney and brain mitochondria. *Rejuvenation research* **12**, 421-434 (2009); published online EpubDec (10.1089/rej.2009.0902).
164. F. P. Rodrigues, C. R. Pestana, A. C. Polizello, G. L. Pardo-Andreu, S. A. Uyemura, A. C. Santos, L. C. Alberici, R. S. da Silva, C. Curti, Release of NO from a nitrosyl ruthenium complex through oxidation of mitochondrial NADH and effects on mitochondria. *Nitric oxide : biology and chemistry / official journal of the Nitric Oxide Society* **26**, 174-181 (2012); published online EpubMar 31 (10.1016/j.niox.2012.02.001).
165. M. Yang, A. K. Camara, B. T. Wakim, Y. Zhou, A. K. Gadicherla, W. M. Kwok, D. F. Stowe, Tyrosine nitration of voltage-dependent anion channels in cardiac ischemia-reperfusion: reduction by peroxynitrite scavenging. *Biochimica et biophysica acta* **1817**, 2049-2059 (2012); published online EpubNov (10.1016/j.bbabio.2012.06.004).